

**NASA
Technical
Paper
2229**

January 1984

NASA
TP
2229
c.1

Correlations of Supersonic Boundary-Layer Transition on Cones Including Effects of Large Axial Variations in Wind-Tunnel Noise

Fang-Jenq Chen,
Ivan E. Beckwith, and
Theodore R. Creel, Jr.



LOAN COPY: RETURN TO
AFWL TECHNICAL LIBRARY
KIRTLAND AFB, N.M. 87117

NASA

**NASA
Technical
Paper
2229**

1984

TECH LIBRARY KAFB, NM



0067863

Correlations of Supersonic Boundary-Layer Transition on Cones Including Effects of Large Axial Variations in Wind-Tunnel Noise

Fang-Jenq Chen

*Systems and Applied Sciences Corporation
Hampton, Virginia*

Ivan E. Beckwith and
Theodore R. Creel, Jr.

*Langley Research Center
Hampton, Virginia*



National Aeronautics
and Space Administration

Scientific and Technical
Information Branch

SUMMARY

Transition data on sharp-tip cones in two pilot low-disturbance wind tunnels at Mach numbers of 3.5 and 5 have been correlated in terms of noise parameters with data from several conventional wind tunnels and with data from supersonic flight tests on the Arnold Engineering Development Center 10° transition cone. The noise parameters were developed to account for the large axial variations of the free-stream noise and the very-high-frequency noise spectra that occurred in the low-disturbance tunnels for some test conditions. These two pilot tunnels utilize some new and unique techniques to reduce the free-stream noise levels below those which are present in conventional tunnels. One of these techniques involves the use of boundary-layer suction slots upstream of the throat. By operating these tunnels with the suction off or on, the noise could be varied from high levels, approaching those in conventional tunnels, to extremely low levels. These changing noise levels resulted in transition-onset Reynolds numbers for the cone models that varied from about 2×10^6 to 8.5×10^6 at the same unit Reynolds number. With the boundary-layer bleed off, the cone transition Reynolds numbers increased with unit Reynolds number, similar to the trend in conventional tunnels. With the boundary-layer bleed on, this trend was reversed because of the upstream movement of transition in the nozzle-wall boundary layer and the corresponding increases in stream noise.

The final correlations indicated that transition in the low-disturbance tunnels was dominated by the local stream noise that was incident on the cone boundary layer upstream of the neutral stability point. The correlation results also suggested that high-frequency components of the low-disturbance-tunnel noise spectra had significant effects on transition when the noise was incident on the boundary layer both upstream and downstream of the neutral stability point.

INTRODUCTION

The powerful adverse effect of wind-tunnel noise on boundary-layer transition was clearly established several years ago by the remarkable correlations of Pate and Schueler (ref. 1) and Pate (ref. 2). Reference 1 showed that transition Reynolds numbers on a test model in Tunnel A at the Arnold Engineering Development Center (AEDC) varied inversely with root-mean-square (rms) stream noise levels. The noise was increased above tunnel ambient levels by a factor of about 4 when the test region was enclosed with a cylindrical shroud and the boundary layer on the inside wall of the shroud was turbulent. The apparent universal dependence of transition on tunnel noise was then conclusively demonstrated (ref. 1) by the accurate correlation between transition Reynolds numbers (for the end of transition on planar models) and noise-dependent parameters in nine different wind tunnels at Mach numbers from 3 to 8. These correlating parameters were the mean skin friction and displacement thickness of the tunnel-wall turbulent boundary layers and the test-section circumference. Although stream noise data were not yet available in all these tunnels, the parameters used in the correlation were related to the tunnel noise by inference from the earlier analysis and measurements in the 20-Inch Tunnel at the Jet Propulsion Laboratory (JPL) by Laufer in references 3 and 4.

In reference 2, Pate successfully applied the same correlating parameters to transition on sharp-tip cones in 11 different tunnels over the Mach number range from 3 to 14. From these data and correlations, Pate also showed (ref. 2) that the ratio of transition Reynolds number for cones to that for planar models decreased from about 2.5 at Mach 3 down to about 1 at Mach 8. This transition ratio also appeared to decrease with an increase in tunnel size, which implies a decrease in the ratio with decreasing tunnel noise.

Stainback first showed in references 5 and 6 that a quantitative relationship exists between wind-tunnel rms pressure levels and transition. The local Reynolds numbers at the onset of transition on sharp cones were correlated directly with the noise measured by a pressure transducer flush with the cone surface underneath the laminar boundary layer. With the local cone Mach number kept at 5 by using different cone angles, the correlations with rms noise levels for data from five different wind tunnels with free-stream Mach numbers ranging from 6 to 20 depended only on the ratio of surface temperature to total temperature and on whether the test gas was air or helium. The helium data at higher local Mach numbers (refs. 6 and 7) were later shown by Pate (ref. 8) to agree with his previous noise-parameter correlation for cones (ref. 2).

Following Morkovin's comprehensive review (ref. 9) of the high-speed transition problem and his recommendation for the development of a low-noise hypersonic tunnel (based in part on the revelations of Pate and Schueler (refs. 1 and 2)), the Boundary-Layer-Transition Study Group (BLTSG), chaired by Reshotko, formulated a Program for Transition Research (refs. 10 and 11) that included the development of low-disturbance wind tunnels. Progress reports on this part of the BLTSG program by a group of researchers at the Langley Research Center are available in references 12 to 17.

The most recent achievement by this Langley group is the development of a Mach 3.5 pilot low-disturbance tunnel (referred to hereinafter as the Mach 3.5 pilot quiet tunnel (PQ tunnel)) that exhibits very low noise levels in upstream regions of the test rhombus up to a free-stream unit Reynolds number R_∞ of about 7.6×10^5 per inch (refs. 18 and 19). These low noise levels were observed when the corresponding upstream "acoustic-origin" regions of the nozzle-wall boundary layers were maintained laminar. The laminar wall boundary layers occurred only when the turbulent boundary layer in the subsonic approach to the nozzle was removed by suction slots upstream of the throat. When the suction flow was turned off, the subsonic turbulent boundary layer spilled around the slot lips; then, the test stream noise levels and spectral energy at high frequencies increased by large amounts (at the same test condition) because of the resulting change in the nozzle-wall boundary layers from laminar to turbulent flow. The test stream noise levels, spectra, and axial distributions also varied over wide ranges as R_∞ varied from approximately 2.5×10^5 to 1.5×10^6 per inch.

Data obtained on a 5° half-angle cone in this quiet tunnel (ref. 19) showed that transition Reynolds numbers $R_{e,T}$ varied over a wide range in response to the different noise conditions with R_∞ held constant. Besides these large changes in $R_{e,T}$ with R_∞ held constant, the following unique results were also obtained: (1) the highest transition Reynolds numbers ever measured in a wind tunnel at this Mach number, and (2) startling changes in the effect of unit Reynolds number on $R_{e,T}$ (usually characterized by the relation $R_{e,T} \propto R_\infty^n$). In these tests the exponent n varied from 0.5 to large negative values of -1.3, depending on changes in tunnel noise and cone location within the test rhombus. The unit Reynolds number effect observed in conventional wind tunnels, where $n \approx 0.4$, is usually attributed

to decreases in normalized stream noise levels with increasing R_∞ . However, values varying from $n \approx 0$ for the Ludwig Tube Mach 5 Wind Tunnel tests of Krogmann (ref. 20) to $n \approx 0.6$ for the ballistic-range data of Potter (ref. 21) cannot yet be explained (ref. 22).

Transition data obtained previously at the Langley Research Center by Schopper¹ in a Mach 5 pilot quiet tunnel (ref. 16) also showed some unusual trends with R_∞ when the subsonic boundary-layer suction slots were used. However, the variations of $R_{e,T}$ with R_∞ and with the suction off or on were not as extreme as in the Mach 3.5 tests. These smaller variations of $R_{e,T}$ occurred primarily because transition was not obtained on the cone in the Mach 5 tests for the lowest range of unit Reynolds numbers when the nozzle-wall boundary layers were laminar.

The purpose of the present investigation was to determine if the unusual range and trends in transition data obtained in both the Mach 3.5 (ref. 19) and the Mach 5 pilot quiet tunnels can be ascribed to the corresponding unusual range in the levels, spectra, and axial variations of noise in the tunnels. Since detailed boundary-layer probe data are not yet available, the approach used in this investigation is to examine correlations between the measured transition Reynolds numbers and various functions of the measured noise that may characterize the receptivity of the laminar boundary layer on the cone to the axial variations in the tunnel noise and to the noise spectra. Comparisons of the resulting correlations with previous correlation results similar to those of references 23 and 24, which show a quantitative relation between transition and noise levels of the uniform noise fields as measured in conventional wind tunnels and flight, will be used to assess the validity of the proposed correlation functions.

Another matter of practical concern is the extent of the transitional-flow region from the onset to the end of transition. For example, Masaki and Yakura (ref. 25) showed that the extent of the transitional region can have a significant impact on the design of thermal-protection systems for hypersonic vehicles. Harvey and Bobbitt (ref. 26) presented correlations for the ratio of the onset to the end of transition Reynolds numbers from data in conventional wind tunnels and flight. Again, correlations of the quiet-tunnel data will be evaluated by comparison with these and other previous results.

SYMBOLS

A, A'	constants (see eq. (7))
B	constant exponent (see eq. (10))
C	constant (see eq. (1))
F	dimensionless frequency, $2\pi f v_\infty / u_\infty^2$
f	frequency
M	Mach number

¹Proposed NASA CR by M. R. Schopper (now at the David Taylor Naval Ship Research and Development Center, Bethesda, Md.) entitled "Boundary-Layer Transition and Supersonic Wind-Tunnel Noise."

N	noise-correlation parameter (see eqs. (6) and (7))
n	exponent (see eq. (1))
P	function of s (see eqs. (6) and (7))
p	pressure
Q	function of f and s (see eqs. (6) and (7))
q	dynamic pressure, $\frac{1}{2} \rho u^2 = \frac{\gamma}{2} p M^2$
R	unit Reynolds number
$R_{e,T}$	local Reynolds number based on flow distance to transition onset
$R_{e,TE}$	local Reynolds number based on flow distance to transition end
$R_{\Delta s}$	Reynolds number based on length of transition region
s	distance from apex of cone along cone generator
T	absolute temperature
u	streamwise velocity
X	axial distance from nozzle throat
X'	axial distance from cone tip
Y	vertical distance from centerline of tunnel
γ	ratio of specific heats
θ	cone half-angle
μ	Mach angle in free stream
ν	kinematic viscosity
ρ	mass density
σ	standard deviation from least-squares fit

Subscripts:

a	most-amplified frequency
e	local conditions at edge of boundary layer
m	at maximum energy of spectrum
N	location on model of point on lower neutral stability curve

o	stagnation
qt	quiet tunnel
ref	reference
T	transition onset
TE	transition end
t	pitot probe
tip	cone apex
w	wall
∞	free stream

Abbreviations:

B.V.	bleed valve
LRC	Langley Research Center
PQ	pilot quiet
rms	root mean square
T.S.	test section
2-D	two-dimensional

Notations:

\sim	root mean square
-	mean value
< >	average value (see eq. (2))

BOUNDARY-LAYER RESPONSE TO EXTERNAL NOISE

Current Status in Conventional Tunnels

The understanding of supersonic wind-tunnel noise and how its interaction with the laminar boundary layer on test models leads to premature transition has improved significantly since the early investigations of references 1 to 7. The most notable contribution to this improved understanding has been the work of Mack and Kendall (refs. 27 to 31). The importance of this unique joint effort to the research problem of transition in supersonic and hypersonic wind tunnels is emphasized by discussions in the earlier review paper of Morkovin (ref. 9) and in the more recent reviews of Reshotko (ref. 11) and Morkovin (ref. 32). In particular, the "receptivity" of the laminar boundary layer to the wind-tunnel acoustic noise field has been clarified. Thus, in reference 30, Mack describes how his forcing and stability theories may be

combined to calculate the amplification of disturbances in the boundary layer. He assumed that the forcing theory applies up to the neutral stability point for the particular frequency under consideration, and that the stability theory applies downstream of that point. At $M_\infty = 4.5$, the streamwise location of the peak response of the boundary layer to the incident noise, as computed from the forcing theory, is at about the same location as the neutral stability point for the same frequency. The trends of the peak amplification ratios measured by Kendall (ref. 31) within the boundary layer at this Mach number and over a range of frequencies were in good agreement with the combined forcing and stability theory up to the start of nonlinearity, which occurred at a length Reynolds number of about 1.5×10^6 . Transition then followed farther downstream at a length Reynolds number of about 2.25×10^6 for the same tunnel conditions. This good agreement between theory and experiment implies that the tunnel noise enters the boundary layer and is amplified mainly upstream of the neutral stability point, but has little, if any, additional effect downstream of this point.

It is important to emphasize here that the noise field in conventional wind tunnels is spatially uniform. (See ref. 4.) Therefore, the results of Mack and Kendall are of special interest for the present correlation efforts because the noise field was not spatially uniform within the quiet-tunnel test regions. In fact, for some cases the noise levels incident upon this upstream sensitive portion of the model boundary layer were so low that the hot-wire signal was within the range of the instrument noise (ref. 19). These quiet-tunnel data may then be used to determine, at least in a "macroscopic" sense, how transition is affected when tunnel noise is incident upon only those regions of the boundary layer downstream of the neutral point while the upstream, and presumably more sensitive regions of the boundary layer (as indicated by the aforementioned Mack-Kendall results), are deprived of the external-noise input that is present in conventional tunnels.

Review of Quiet-Tunnel Data and Preliminary Assessment of Tunnel-Noise Effects

Before we present the details of the present correlation attempts, we will first review briefly the available quiet-tunnel data. The local Reynolds numbers for the onset of transition are plotted against the local unit Reynolds numbers in figure 1 for all the data from reference 19. These data were obtained in the Mach 3.5, two-dimensional, rapid-expansion nozzle described in the "Introduction." Sufficient transition data from another quiet-tunnel investigation by Schopper² at Mach 5 to show the trends observed are also included in figure 1. Some of these earlier transition data were also published in a review paper by Trimpi (ref. 33). Most of the data reported by Schopper were for the end of transition, so the data shown in figure 1 have been "corrected" to the onset of transition by a procedure to be discussed later. The cross-hatched bands in figure 1 labeled "Flight Data" and "Conventional Wind-Tunnel Data" are identical to those used in reference 19 where the original data sources are referenced. All wind-tunnel data used in figure 1, including the quiet-tunnel data, are for adiabatic wall temperatures on the surface of the test cones. All flight data are for cold-wall conditions with T_w/T_o ranging from about 0.3 to 0.8, except for the data of references 23 and 24 which are for adiabatic wall temperatures.

²See footnote 1 on page 3.

The quiet-tunnel data of Schopper were obtained in the Mach 5, slotted, rapid-expansion, axisymmetric nozzle (refs. 16 and 34), which was developed and tested at the Langley Research Center as part of the quiet-tunnel development program of the Boundary-Layer-Transition Study Group. This nozzle was equipped with a boundary-layer removal slot upstream of the throat. The function and operation of this slot, by means of bleed-control valves, was similar to that in the Mach 3.5 nozzle of reference 19. The available measurements of noise levels and spectra in the Mach 5 nozzle are given in references 16 and 34 to 36. The spectra and axial distributions of the noise in this nozzle were similar to those in the Mach 3.5 nozzle (refs. 18 and 19). That is, the noise levels in the upstream region of the test rhombus were about an order of magnitude lower than those near the nozzle exit, and the noise power spectra with bleed valves closed were characterized by peak energies at high frequencies from 40 to 80 kHz (ref. 35). Laminar boundary layers were observed on the wall of this Mach 5 nozzle at significant distances downstream of the throat when the bleed valves were open, but they were observed only up to $R_{\infty} \approx 3.8 \times 10^5$ per inch, which was too low to obtain transition (with laminar boundary layers on the nozzle wall) on the 8-in-long cone used for those tests. Nevertheless, representative transition data from this earlier investigation (of Schopper) with bleed valves both open and closed are included in figure 1 for comparison with the more recent quiet-tunnel data of reference 19. The agreement between the two sets of quiet-tunnel data at different Mach numbers and in different nozzles is considered remarkable in view of the unusual trends and levels of these data as emphasized in the following discussion. The apparent lack of dependence of $R_{e,T}$ on Mach number may simply indicate the dominant effect of the similar noise conditions in the two nozzles.

Figures 1(a) and (b) show the transition data with bleed valve open and with the cone models at upstream and downstream locations, respectively. The peculiar decreasing trends of $R_{e,T}$ with increasing R_e , mentioned previously, are apparent in both figures for $R_e > 7 \times 10^5$ per inch. The "unit Reynolds number effect" in conventional wind tunnels is often expressed in the form

$$R_{e,T} = CR_e^n \quad (1)$$

where C is a constant and the exponent n is usually a positive constant. Typical values for n vary from about 0.2 to 0.4, presumably because of the decreasing trends of the normalized rms pressure fluctuations with R_{∞} usually observed in the test sections. However, values of nearly zero have been recorded in some wind tunnels. (See refs. 9 and 20.) The larger values for n of about 0.6 observed in ballistic ranges (refs. 21 and 37), where stream disturbance levels are extremely small, are one of the major enigmas in transition research as pointed out by Morkovin. (See ref. 32.) The overall unit Reynolds number trend of the flight data shown in figure 1 is $n \approx 0.9$ which, again, is inexplicable in terms of the presumably even smaller stream disturbances in these flight tests. Other factors, such as variable wall temperatures, may be involved in this apparent data trend with unit Reynolds number. Furthermore, some data from single flight tests used in figure 1 (see ref. 19) exhibit values of n near unity, which suggests a fixed transition location due to a local surface defect on the model. In view of these previous results and, especially, the previous results from conventional wind tunnels, the negative values for n of about -1.3 and -1.0 for $R_{\infty} > 7 \times 10^5$ per inch in figures 1(a) and (b), respectively, are certainly unique. These trends which, to our knowledge, have never

before been observed in any wind tunnel, have already been qualitatively related (ref. 19) to changes with R_∞ in the levels, spectra, and axial distributions of the tunnel noise.

Typical axial distributions from reference 19 of the normalized rms static-pressure fluctuations measured along the nozzle centerline are shown in figure 2. To help provide a qualitative indication of the dependence of transition on the noise distributions, a portion of the nozzle contour with the cone positioned in its two test locations is included in the upper part of figure 2. The Mach lines that outline the theoretical uniform test-flow rhombus are also shown. When the cone apex is at $X = 5$ in., it is slightly upstream of this test-rhombus tip on the centerline. However, mean-flow pitot-pressure surveys reported in references 18 and 19 show that the mean flow is essentially uniform to $X = 5$ in. The symbols plotted on the cone surface in figure 2 represent the measured locations of transition at selected values of R_∞ corresponding to noise data in the lower part of the figures where the same symbols denote test conditions at about the same values of R_∞ . Thus, for example, at $R_\infty \approx 2.5 \times 10^5$ per inch with bleed valve open (square symbols in fig. 2(a)), transition does not occur on the cone even though the noise levels increase to about 0.8 percent near the end of the cone when it is positioned in the downstream test location. At $R_\infty \approx 5.3 \times 10^5$ per inch (triangle symbols), transition does occur on the cone but in about the same spatial region in the nozzle ($X \approx 17.5$ to 20.2 in.) for both test locations of the cone. In figure 2(b), the behavior of transition at $R_\infty \approx 7.9 \times 10^5$ per inch is similar to that just noted; but at $R_\infty \approx 12.4 \times 10^5$ per inch, the average distance to transition from the cone tip is about 3 in. at both test locations since the noise has then increased above the extremely low "laminar" levels ($\bar{p}_\infty/\bar{p}_\infty < 0.1$ percent) all the way to the apex for both test locations. From these examples, it is apparent that transition on the cone is strongly affected by the location in the test flow where the noise increases from very low levels to higher levels caused by transition from laminar to turbulent flow in the nozzle-wall boundary layer at the upstream acoustic origins. (See ref. 19.) This "transitional" location within the test flow moves upstream with increasing R_∞ and apparently has an increasing effect on transition as it approaches the more sensitive regions of the cone boundary layer in the vicinity of, or upstream of, the lower neutral stability point, which is roughly 1 in. from the cone tip for these test conditions. Clearly, the reverse trends of $R_{e,T}$ with R_e in figures 1(a) and (b) are related to the differing receptivities to tunnel noise of the regions in the cone boundary layer upstream and downstream of the lower neutral stability points.

Also to be noted in figures 1(a) and (b) are the high values of $R_{e,T}$ obtained in the Mach 3.5 investigation where a 15-in-long cone was used. Some of these $R_{e,T}$ values are not only higher than any measured before in wind tunnels at this Mach number but they are also in agreement with the lower range of values from flight data. Although stream noise or disturbance measurements are not usually available for flight tests, these disturbances are generally believed to be quite small. Sources for the flight data used in figure 1 are given in reference 19 and include the recent high-quality data of Dougherty and Fisher (refs. 23 and 24). They obtained both transition and stream-disturbance data over the Mach number range from 0.4 to 2.0, but only their data for $M_e > 1.6$ have been used in figure 1.

The bleed-valve-closed transition data are shown in figures 1(c) and (d), again for the same two axial locations of the cones. For these higher tunnel-noise conditions, the quiet-tunnel data are generally closer to the data for conventional wind tunnels, but they range from somewhat above to considerably below the conventional-tunnel data. (The sources for the conventional-tunnel data used in fig. 1 are given

in ref. 19 and are restricted to the smaller tunnels and to the range of Mach number M_e from 2.5 to 4.4.) Although the overall variation of $R_{e,T}$ with R_e is similar to that for the conventional-tunnel data, there appear to be regions of significantly lower values of $R_{e,T}$ in the ranges of unit Reynolds number R_e from approximately 5×10^5 to 6×10^5 per inch in figure 1(c) and from approximately 3×10^5 to 5.5×10^5 per inch in figure 1(d). These low values of $R_{e,T}$ are again related to the tunnel-noise distributions which are shown in figures 2(c) and (d) for the bleed-valve-closed condition. Thus, the large "transitional" peaks in noise levels for $R_e \approx 2.5 \times 10^5$ and 5.3×10^5 per inch (fig. 2(c)) in the upstream regions of the test rhombus are probably the main cause of these low values of $R_{e,T}$.

When R_e is increased above 7.5×10^5 per inch, the values of $R_{e,T}$ and the trends of $R_{e,T}$ with R_e shown in figures 1(c) and (d) are in good agreement with conventional-tunnel data, probably because the noise field is more nearly uniform in the upstream regions of the test rhombus. However, since these noise levels are still quite low, this agreement in the values and trends of $R_{e,T}$ with conventional-tunnel data does not result in agreement with the accepted noise correlations of transition data in conventional tunnels. As will be seen in the next section of this report, agreement with the previous noise correlations can be obtained only by accounting for the markedly higher frequency peaks in the noise spectra of the quiet tunnels. With this review of the quiet-tunnel transition and noise data, we are now ready to formulate some proposed quantitative noise parameters that will be considered in the following correlations.

NOISE FUNCTIONS AND APPLICATIONS TO $R_{e,T}$ CORRELATIONS

General Forms

Figure 3 is presented to show that the quiet-tunnel data do not correlate with the other data in the figure in terms of the rms average noise parameter $\langle \tilde{p}/\bar{q} \rangle$. Apparently, special noise-related parameters will be required to account for the effects on transition of the unique axial distributions and frequency content of the quiet-tunnel noise. The Reynolds numbers for the onset of transition are plotted in figure 3 against the "average" noise incident upon the cone from the tip to transition onset for the two sets of quiet-tunnel data (ref. 19 and Schopper's Mach 5 data). The average noise is defined as

$$\left\langle \frac{\tilde{p}}{\bar{q}} \right\rangle = \frac{1}{s_T} \int_0^{s_T} \frac{\tilde{p}}{\bar{q}} ds \quad (2)$$

Since noise data are not available for each transition data point from reference 19 shown in figure 1, or for all of Schopper's Mach 5 data, average values of $R_{e,T}$ for the upstream and downstream test locations have been selected for the several unit Reynolds numbers for which noise data were obtained with the bleed valve open and closed. These selected values of $R_{e,T}$ and the corresponding test conditions are listed in table I for both quiet-tunnel investigations. For comparison, the transition-onset Reynolds numbers from several conventional wind tunnels (refs. 5, 6, 38, and 39) and from flight (ref. 40) are also plotted in figure 3 against the corresponding measured noise which is assumed to be uniform along the entire cone for these data. Noise data from references 4 and 41 are used with corresponding transition data from references 39 and 38 (AEDC Tunnel A), respectively. These data from conventional tunnels and from this recent flight experiment will be used throughout this report as a representative set of established data for a reference standard to

develop the required correlation parameters. To reduce the number of variables that complicate correlation efforts, these data have been limited to the local Mach number range from 1.5 to 5.0 and, except for the data from references 5 and 6, to adiabatic wall temperatures.

Equation (2) was used in a first attempt to account for the axial variations in noise for the quiet-tunnel data. Also, when \tilde{p}/\bar{q} is constant, which applies for conventional wind-tunnel data and flight data, that constant value is recovered. For all hot-wire data, \tilde{p}/\bar{q} is defined as

$$\frac{\tilde{p}}{\bar{q}} = \frac{\tilde{p}_{\infty}}{\frac{\gamma}{2} M_e^2 \bar{p}_{\infty}} \quad (3)$$

When the noise data are obtained from pressure transducers flush with the model surface, then \tilde{p}/\bar{q} is defined as

$$\frac{\tilde{p}}{\bar{q}} = \frac{\tilde{p}_e}{\frac{\gamma}{2} M_e^2 \bar{p}_e} \quad (4)$$

These equivalent forms are based on comparisons of both types of data from several different wind tunnels in the review paper by Laderman (ref. 42), where it was shown that values of $\tilde{p}_{\infty}/\bar{p}_{\infty}$ from hot-wire data are approximately the same as values of \tilde{p}_e/\bar{p}_e from pressure transducers on cones underneath the laminar boundary layer when the tunnel flow conditions are the same. Use of the local cone Mach number M_e , rather than the free-stream Mach number M_{∞} , in the dynamic-pressure parameters as defined previously is based on the good correlation results of Harvey (ref. 43), where a similar definition of \bar{q} was used. For the flight data of Fisher and Dougherty (ref. 40), the normalized rms noise parameter is defined herein as

$$\frac{\tilde{p}}{\bar{q}} = \frac{\tilde{p}_t}{\frac{\gamma}{2} M_e^2 \bar{p}_t} \quad (5)$$

This definition is based on comparisons of hot-wire and pitot-pressure measurements in references 19, 34, and 35, where it was shown that \tilde{p}_t/\bar{p}_t is approximately equal to $\tilde{p}_{\infty}/\bar{p}_{\infty}$ when the peak energy in the pressure-fluctuation spectra is below 30 to 40 kHz. This limitation obviously depends on the probe size, the transducer resonance properties, and other test conditions; however, the flight data of reference 40 easily qualify in all respects since the measured peak energy was below 2 kHz.

Figure 3 shows that the flight data from reference 40 and the data from conventional wind tunnels are correlated fairly well with this noise parameter within a "scatter" band of about ± 20 percent. The same type of correlation with the same scatter was obtained previously by Dougherty and Fisher (refs. 23 and 24) for the AEDC transition cone used for the flight tests and in 23 wind tunnels over the Mach

number range from 0.25 to 4.60. Data from three additional wind tunnels (refs. 5, 6, and 39) not used in that previous correlation are included in figure 3; however, the range of Mach number M_e is restricted here from approximately 1.5 to 5.0. Since the quiet-tunnel data points show no "self-correlation" of their own and do not correlate with the other conventional wind-tunnel data or flight data, it is now clearly evident that a simple average of the incident rms noise is not a correlating parameter for the quiet-tunnel data. Most quiet-tunnel data from reference 19 are not within the correlation scatter band of the other data, except for a few points at the highest values of $R_{e,T}$ with the bleed valve open. These few data points are in excellent agreement with the flight data.

A modified noise-correlation parameter of the following general form is now proposed:

$$N = \frac{A}{s_T} \int_0^{s_T} \frac{\tilde{p}}{\tilde{q}} P(s) Q(f,s) ds \quad (6)$$

where the definitions for \tilde{p}/\tilde{q} from equations (3) to (5) will be retained and used as required by the type of noise data available for each set of transition data. The function $P(s)$ is intended to indicate whether the cone boundary-layer response to the axial variations of the rms tunnel noise is dependent on the distance from the cone tip. Of course, in the absence of "microscopic" data within the cone boundary layer, the only way to arrive at a judgment concerning the validity of this type of "receptivity" function is, first, to find out, essentially by trial and error, if a chosen function improves the self-correlation of the quiet-tunnel transition data and then, second, see if the degree of correlation with the other data is also improved. The other function ($Q(f,s)$) in equation (6) will be used in much the same way as the P function but for the purpose of characterizing the effects on the correlation of selected properties of the noise spectra, such as frequency or wave number. These properties of the noise spectra are already known (ref. 19) to be much different from those in conventional wind tunnels. The parameter A is simply a constant that will be used to normalize the integrals of P and Q so that when \tilde{p}/\tilde{q} is constant, the desired relation $N \equiv \tilde{p}/\tilde{q}$ will be recovered. This normalizing feature will facilitate comparisons with the correlation for conventional tunnels and the flight data (ref. 40) as presented in figure 3.

The selection of these functions can benefit from the Mack-Kendall results previously mentioned. Thus, the combined forcing and stability theories (refs. 30 and 31) suggest, first of all, that equation (6) should be divided into two terms to provide for differing sensitivities of the cone boundary layer to the incident noise at locations upstream and downstream of the neutral stability point. Equation (6) is then written as

$$N = \frac{1}{s_T} \left(A \int_0^{s_N} \frac{\tilde{p}}{\tilde{q}} Q ds + A' \int_{s_N}^{s_T} \frac{\tilde{p}}{\tilde{q}} P Q ds \right) \quad (7)$$

where $P = 1$ has been used from the cone apex to the neutral stability point to account crudely for the forced amplification in the boundary layer of the incident noise in this region. (See refs. 30 and 31.)

Self-Correlation of Mach 3.5 Quiet-Tunnel Data

The next step in deriving the correlation functions is to try some likely functions for P in the second term of equation (7), while using $Q = 1$ and $A = 1$ to see if any degree of self-correlation can be obtained for the quiet-tunnel data. Besides the use of $A'P = 1$, as applied in equation (2) and figure 3, three other arbitrary functions have been used as follows:

$$A'P = \frac{\pi}{2} \cos\left(\frac{\pi}{2} \frac{s - s_N}{s_T - s_N}\right) \quad (8)$$

$$A'P = 2 \frac{s_T - s}{s_T - s_N} \quad (9)$$

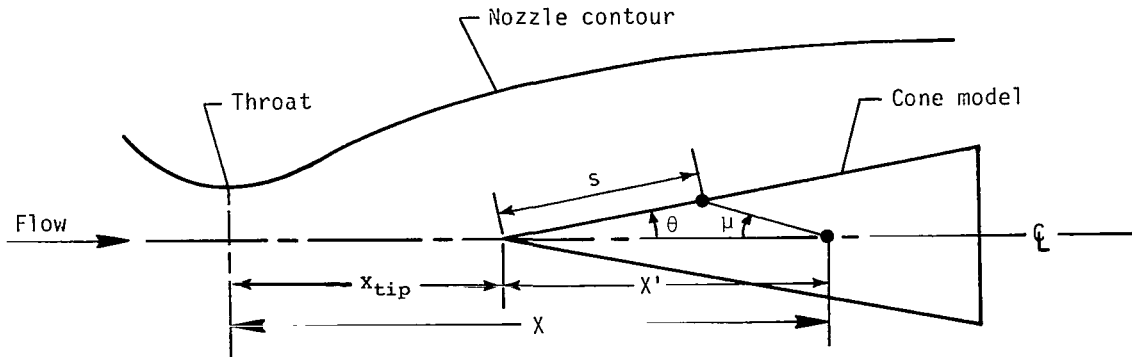
and

$$A'P \approx B \exp\left(-B \frac{s - s_N}{s_T - s_N}\right) \quad (10)$$

The approximate form of equation (10) results because $B > 10$ in this investigation. The effects of using the functions in equations (8), (9), and (10) on the self-correlation of the Mach 3.5 quiet-tunnel data from reference 19 are shown in figures 4(a), (b), and (c), respectively. The values of s_N used as limits for the integrals of equation (7) are listed in table I(a). These values, which were estimated from linear-stability calculations made by Malik with his computer code of reference 44, were applied to the present conditions for the most-amplified frequencies over the range of typical values of $R_{e,T}$. Schopper's Mach 5 data were not used here because values of s_N were not available for the conditions in those tests. The values of β/\bar{q} and f_m used for the transition data from reference 19 are given in table II as functions of X . The corresponding selected average values of $R_{e,T}$ are listed in table I. The noise was measured along the nozzle centerline at the indicated X stations (table II). To determine the location of that noise incident upon the cone surface, we have assumed that these centerline values are projected in the upstream direction along a Mach line in accordance with the physical requirement and experimental observations (ref. 19) that noise is propagated along Mach lines in supersonic flow. The relation between the X location of the measured centerline noise levels and spectra (table II and fig. 2) and the corresponding location on the cone surface where that noise interacts locally with the cone boundary layer is then given by

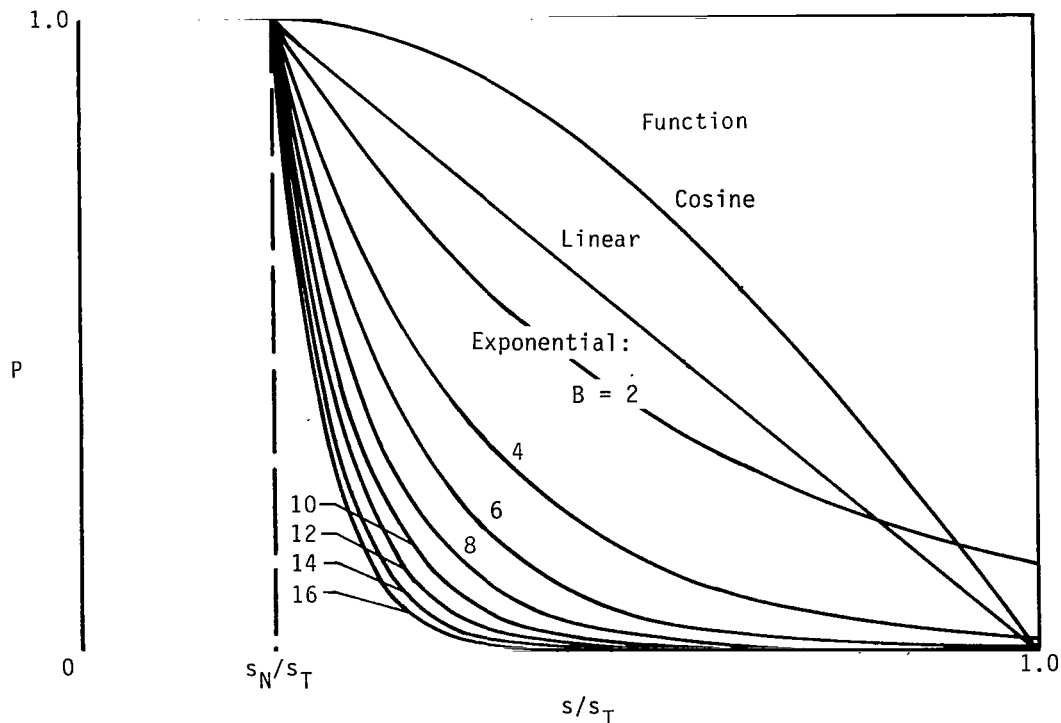
$$s = \frac{X'}{\cos \theta + \frac{\sin \theta}{\tan \mu}} \quad (11)$$

as illustrated in the following sketch:



Figures 4(a) and (b) show how the cosine and linear functions defined by equations (8) and (9), respectively, improve the self-correlation of the quiet-tunnel data compared with the unmodified average noise parameter of equation (2) as shown in figure 3. The standard deviation σ , from the least-squares straight-line fit shown in all the correlation figures, may be used as a comparative index of the "quality" of the correlations. Thus, the linear function appears to be slightly better than the cosine function. If this trend of improved correlations with decreasing values of P in the region from s_N to s_T continues, then we would have expected the exponential function (eq. (10)) to give better results than the cosine and linear functions with moderate values of B around 3 or 4. However, the large value of $B = 12$ was required to minimize σ to the value of 8.1×10^5 , as shown in figure 4(c).

To provide the reader with a visual impression of how much the various P functions modify the local noise parameter \bar{p}/\bar{q} (which also varies with s , but only for the quiet-tunnel data), the following sketch may be consulted:



Thus, when $B = 12$, the effect of the local noise on the self-correlation and, by implication, on the location of transition is nearly zero about halfway between s_N and s_T . The total effect on the noise in the region upstream of s_N depends not only on the local noise levels there, which from figure 2 may be very small, but also on the ratio of s_N/s_T , which varied from about 0.08 to 0.32 for the selected data used here. (See table I.)

The flight data and conventional-tunnel data (which are plotted the same as in figure 3 because $N = \langle \tilde{p}/\tilde{q} \rangle$ when \tilde{p}/\tilde{q} is constant) are also shown in figure 4 for comparison. In figure 4(c), the self-correlation of the quiet-tunnel data is obviously much better than that obtained with the other P functions; however, most of the bleed-valve-open data have been shifted by varying amounts to the left, whereas the bleed-valve-closed data have generally shifted by smaller distances or not at all. Thus, there is now very poor correlation between the quiet-tunnel data and all other data. This poor correlation is apparently caused by the exponential type of P function used and its normalizing constant, which reduces the magnitude of N by large amounts when most of the noise is incident on the boundary layer downstream of the neutral point. However, since this function improves the self-correlation of the quiet-tunnel data significantly, we conclude that it does provide a reasonably good model of the boundary-layer response to the variable external noise and shows how that noise then affects transition.

This result might have been expected from Mack's combined forcing and stability theory (ref. 30) and the good agreement of the predicted boundary-layer-disturbance amplitudes with Kendall's data (ref. 31). The assumption was made in this theory that the tunnel noise entered the boundary layer only upstream of the neutral stability point. The direct application of this assumption to the quiet-tunnel data would reduce equation (7) to the form

$$N = \frac{A}{s_N} \int_0^{s_N} \frac{\tilde{p}}{\tilde{q}} Q \, ds \quad (12)$$

We then set $Q = 1.0$ and $A = 1.0$, as before, to consider only the self-correlation of these data. The result is shown in figure 5 where the same $R_{e,T}$ values from table I are plotted against N , as now defined by equation (12). The value of σ is reduced to 5.3×10^5 , which is a significant improvement over any of the other P functions used in figure 4. It follows that Mack's assumption (ref. 30) appears to be confirmed for the present data. These results imply that only the rms levels of tunnel noise incident on the boundary layer upstream of s_N have any effect on transition. However, this implication cannot be entirely correct for the present data since, as mentioned previously in the discussion of figures 2(a) and (b), the values of $R_{e,T}$ were reduced significantly by simply moving the cone downstream within the tunnel noise field at the two unit Reynolds numbers of 5.3×10^5 and 7.9×10^5 per inch. For these two unit Reynolds numbers, the rms levels of noise incident upon the boundary layer upstream of s_N were always quite small.

From the reasonably good self-correlation results obtained by using both terms of equation (7), as shown in figure 4(c), it may then be concluded that the noise incident on the boundary layer downstream of the neutral point does have some effect on the location of transition, presumably by interacting with the unstable Tollmien-Schlichting waves. However, from the results shown in figure 5, it may also be concluded that the noise incident on the boundary layer upstream of s_N probably has a dominant effect on transition. Any apparent conflict here can be resolved only by "microscopic" probing of the model boundary layer similar to the work of Kendall

(ref. 31). That is, detailed experimental studies will be needed of the response ("receptivity") of the boundary layer, in terms of local amplitudes and frequencies, to the large axial variations in levels and spectra of the external disturbances in this tunnel. These studies would be designed to reveal how the external disturbances excite or modify the internal Tollmien-Schlichting waves of the boundary layer.

Correlation of Quiet-Tunnel Data With Other Data

Comparison of figure 4(c) or 5 with figure 3 shows that none of the quiet-tunnel data correlate with the other data in terms of the effective noise parameter N when the function Q equals 1. This result implies that the critical rms noise levels which are incident on the more-sensitive upstream regions of the cone boundary layer, where the most "damage" is done toward promoting early transition, are much smaller (by about an order of magnitude) than the corresponding noise levels in conventional tunnels or in flight. Therefore, some other property of the quiet-tunnel noise, that is not present in conventional tunnels, must be causing the poor overall correlation in figure 4(c).

Reshotko pointed out (ref. 45) that apparent discrepancies in transition data obtained in different wind tunnels, such as the effect of wall cooling, could be accounted for by differences in a characteristic dimensionless frequency or wavelength of the disturbance environment as predicted by stability theory. He therefore cautioned that spectral components of available disturbances, which are relevant to instability-amplification processes, should be carefully considered in the evaluation of experimental results. Accordingly, in an attempt to characterize one notable difference between the frequency spectra in the quiet tunnels and those of conventional tunnels, we define the frequency function Q in equation (7) as

$$Q = \frac{(F_m R_\infty)_{qt}}{(F_m R_\infty)_{ref}} \quad (13)$$

which is the ratio of a characteristic wave number in the quiet tunnels to that found in conventional tunnels. For the present purposes, F_m is selected as the dimensionless frequency of the peak energy in the noise spectra. This value is multiplied by the corresponding free-stream unit Reynolds number. The product of $F_m R_\infty$ is then a characteristic wave-number parameter rather than a frequency parameter. From available published spectra for two conventional tunnels and from the flight tests of Fisher and Dougherty (ref. 40), it was found that this product was nearly constant at the value of 0.25 per inch. The sources and values of F_m and R_∞ used to arrive at this value are listed in table III. For the present correlation attempts, we have therefore assigned this value to all other conventional wind tunnels and to other flight conditions for the data to be used. (These are the same data already presented in figs. 3 and 4.) With this definition, the frequency parameter Q is unity for all these data, and so the required normalization of that function is satisfied.

In the quiet tunnels, $F_m R_\infty$ is a function of X and R_∞ , as shown in figures 6(a) and (b) for the bleed valve open and closed, respectively. The corresponding frequencies and the F_m values are also given in table II. All spectral data obtained on the centerline of the Mach 3.5 quiet tunnel have been used here. Some of these data at $R_\infty \approx 5.3 \times 10^5$ and 7.9×10^5 per inch were published in reference 19. For $R_\infty \approx 2.5 \times 10^5$ per inch with bleed valve open, some spectral

data obtained with pitot-pressure probes at small values of X from reference 18 were also used. Only three values of F_m for the Mach 5 quiet tunnel were available from published spectra (ref. 35). These spectra were for the bleed valve closed, and the corresponding $F_m R_\infty$ values are included in figure 6(b). Obviously, the selection of definite peaks from any of these spectra during the experiments was not always very precise and the spectral distributions were not always repeatable. Thus, the data shown in figure 6 should be considered as indicative of only approximate magnitudes and trends as perhaps would be apparent from the rather large scatter of the data.

In view of these limitations on the spectral data and values of Q , as well as questions about the basic concepts involved, it came as a surprise to obtain the overall good correlation between the quiet-tunnel data and the other data, as displayed in figure 7. Here, N is computed from both terms of equation (7) with $A = 1$, $A'P$ is defined by equation (10), and Q is defined by equation (13). This "good" correlation (compare $\sigma = 7.0 \times 10^5$ from fig. 7 with $\sigma = 6.6 \times 10^5$ from the reference data in fig. 3) emphasizes the importance of noise spectra in these quiet-tunnel transition data.

One possible reason for the good correlation shown in figure 7 is that the most-amplified frequencies, which were computed by Malik for the present conditions with his linear-stability code (ref. 44), gave values of $F_a R_\infty$ that were in the range of the peak values used in the correlations. Malik's results are given in the following table:

$R_e/\text{in.}$	$X'_T/\text{in.}$	$R_{e,T}$	Most-amplified $f_a, \text{ kHz}$	F_a	$F_a R_\infty/\text{in.}$
7.47×10^5	10.9	8.19×10^6	77	2.54×10^5	18.3
5.06	13.4	6.81	64	3.11	15.2
2.41	14.5	3.51	30	3.06	7.1

By comparing these values of $F_a R_\infty$ with the maximum experimental values of $F_m R_\infty$ in figure 6, it is clear that high levels of disturbance energy at the most-amplified frequencies would be available in the quiet tunnels, except in the upstream regions of the test rhombus for the bleed valve open at the two lowest values of R_∞ (fig. 6(a)) and at the lowest unit Reynolds number for the bleed valve closed (fig. 6(b)).

Another possible reason, or "explanation," for the apparent direct influence of dominant stream-disturbance wave numbers on transition, as implied by the correlation of figure 7, may be developed as follows: From a correlation of experimental data for the Reynolds number based on length of the transition zone with the onset transition Reynolds number, Dhawan and Narasimha (ref. 46) derived a relation between transition Reynolds number and the average production rate of turbulent spots. From an optical study of turbulent spots at a Mach number of 1.96, Spangenberg and Rowland (ref. 47) showed that the Reynolds number at the point of origin of the spots varied with their production rate in such a way as to suggest that the spots may have developed from Tollmien-Schlichting (TS) waves. More recently, Chen and Thyson (ref. 48) utilized transition data for Mach numbers up to 5 in the derivation of a relation similar to that of reference 46 between the turbulent-spot-formation rate and transition Reynolds number. They next assumed that the spot-formation rate (per unit time

and unit spanwise distance) was proportional to the ratio of the input disturbance frequency and the spanwise wavelength of three-dimensional structures which have been observed to evolve from TS waves. They computed this spanwise wavelength from the experimental streamwise length of the transition zone and the spot-growth properties. Their predicted trends of input disturbance frequency with transition Reynolds number then agreed with trends from stability theory. It may be tentatively concluded that transition onset is related to the turbulent-spot-formation rate which is determined by the most-amplified TS frequency and the spanwise periodicity of the three-dimensional distortion of TS waves. The present correlation results with Q included, as defined by equation (13), may also indicate that mechanisms of this type are involved in the transition process. Obviously, detailed experimental data are required to establish these possibilities.

It is appropriate to conclude this section with one additional comment on the use of equation (7) in regard to the two terms which allow distinctly different treatment of the regions upstream and downstream of the neutral stability point. Figure 5 showed the result of using only the upstream term of equation (7) to test the self-correlation capability of that term. As a sequel to that result, we return to equation (12), which is a more-general form of that upstream term, and insert the Q function as given by equation (13). The result of this exercise (the figure will not be included here) was an overall correlation with $\sigma = 8.8 \times 10^5$ (compared with $\sigma = 7.0 \times 10^5$ for fig. 7) and with some of the quiet-tunnel data points rather far removed from the correlation line. This suggests that the high-frequency noise components may be more effective downstream of the neutral point than upstream of that point in terms of changing the transition location.

Self-correlation of all quiet-tunnel data.— As mentioned previously, values of s_N were not available for the Mach 5 quiet-tunnel data. However, since a few spectra were available, it is of interest to see if the Q function of equation (13) will also improve the overall correlation of the Mach 5 data as compared with that of figure 3. Therefore, we return to equation (6) and first consider the self-correlation of all the quiet-tunnel data with $Q = 1$, $A = 1$, and the exponential form of equation (10) for the function P . The minimum value for $\sigma = 6.7 \times 10^5$ was obtained with $B = 14$, and the results are shown in figure 8(a). We conclude that the exponential P function works quite well for both sets of quiet-tunnel data.

Figure 8(b) shows the least-squares straight-line fit to the Mach 3.5 data only for which $\sigma = 5.8 \times 10^5$ with $B = 13$. This value of σ should be compared with the lowest value of $\sigma = 5.3 \times 10^5$, as obtained previously for the Mach 3.5 data using equation (12) (with $Q = 1$ and $A = 1$) as plotted in figure 5. From this comparison, it is apparent that the exponential form of P used for the integration from the cone apex to s_T is nearly as effective as the use of $P = 1$ applied from the apex to s_N only. This result shows again that the noise incident on the cone boundary layer downstream of the neutral stability point does affect transition. Furthermore, the noise appears to have an exponentially decreasing effect on transition as that point is approached.

Application of Q function to all quiet data.— We next insert into equation (6) the Q function, as defined in equation (13), and use the exponential P function to test the correlation of both sets of quiet-tunnel data with all other data. The result is shown in figure 8(c) where the minimum σ of 7.4×10^5 was obtained with $B = 10$. Again, this minimum σ is almost as low as the value of $\sigma = 7.0 \times 10^5$ obtained with the double-term form given by equation (7) and plotted in figure 7.

From these results, we may conclude that for practical purposes, the single-term form for N given by equation (6) is about as effective as the double-term form of equation (7).

CORRELATIONS FOR THE TRANSITION-REGION LENGTH

All Data

Dhawan and Narasimha (ref. 46) showed that the Reynolds number based on the length of the transition region $R_{\Delta s}$ increased with increasing transition Reynolds number at about the same rate for widely different conditions in subsonic and supersonic wind tunnels. From a correlation equation for these data, they calculated the average rate of formation of turbulent spots which varied inversely with transition Reynolds number to about the 1.6 power. If the rate of turbulent-spot formation depends on the wind-tunnel disturbance levels and spectra, some correlation between $R_{\Delta s}$ and the tunnel disturbances might be expected.

Harvey and Bobbitt (ref. 26) plotted the ratio $R_{e,T}/R_{e,TE}$ from the AEDC cone data (refs. 39 and 41) against the rms noise parameter $\bar{p}_{\infty}/\bar{q}_{\infty}$. Since

$$\frac{R_{e,T}}{R_{e,TE}} = \left(1 + \frac{R_{e,\Delta s}}{R_{e,T}} \right)^{-1}$$

a correlation between this transition ratio and the same noise parameter would also be expected. However, the Mach number range for these data used in reference 26 was from about 0.2 to 3.5, which may have accounted for the relatively poor correlation shown there because the noise-generating mechanisms and noise-frequency content in subsonic and transonic tunnels are entirely different from those in supersonic tunnels (ref. 49). Thus, for the present purposes, we have restricted the range of Mach number M_e from 1.5 to 5. The ratio s_T/s_{TE} (which, for sharp cones in supersonic flow, is equal to $R_{e,T}/R_{e,TE}$) is plotted against N in figure 9, where N is defined by equation (6). The minimum value of σ is 0.078 for which a value of $B = 13$ was required as compared with $B = 10$ in figure 8(c). This result suggests that the ratio s_T/s_{TE} should correlate directly with $R_{e,T}$ about as well, since the same noise function also correlated $R_{e,T}$ with N . Accordingly, all data are plotted against $R_{e,T}$ in figure 10. Here, σ is equal to 0.070, which appears slightly better than the correlation of s_T/s_{TE} against N in figure 9. However, the values of σ for figures 9 and 10 may not be directly comparable because of the larger number of data points used in figure 10. Nevertheless, from these results, it may be concluded that the ratio s_T/s_{TE} for sharp cones in supersonic flow correlates directly with $R_{e,T}$ about as well as with the noise parameter N defined by equation (6). The physical implication of this conclusion is simply that the same noise parameters that correlate $R_{e,T}$ also provide a reasonable correlation of the length of the transition region.

Mach 5 Quiet-Tunnel Data

As mentioned previously, most of the transition data from the Mach 5 quiet tunnel reported by Schopper were for the end of transition. This occurred not only because of the lack of onset data but also because the reliability of the onset data

was poor as a result of heat-conduction problems related to the test procedures and conditions. Also, there was a heat-sink region between the upstream and downstream thermocouple locations which sometimes interfered with the reliable location of transition.

An assessment of the Mach 5 noise data indicated that in the range of test conditions where transition was on the 8-in-long model ($Re > 6 \times 10^5$ per inch), the axial distributions and spectral characteristics of the noise were similar to those in the Mach 3.5 quiet tunnel with the bleed valve closed. Accordingly, the data of Schopper for the end of transition were corrected to the onset by using the dashed and solid lines shown in figure 11. These lines are the least-squares fits to the Mach 3.5 data for the bleed valve closed with the cone in the two test positions. The dashed line is for the forward position of the cone, which was applied to the Mach 5 data with $X_{tip} = 5.7$ in., and the solid line is for the downstream location, which was applied to the Mach 5 data with $X_{tip} = 7.6$ in. Later on, several plots of the original recovery-temperature data for the Mach 5 tests were obtained. Values of s_T/s_{TE} from these plots by the straight-line-fairing technique described in reference 19 are also plotted in figure 11, which indicates that reasonable agreement with the Mach 3.5 data was obtained. On account of the similar noise conditions in the two quiet tunnels, this agreement justifies the correction procedure just described.

CONCLUDING REMARKS

Transition data on sharp-tip cones obtained previously in two low-disturbance wind tunnels at Mach numbers of 3.5 and 5 were affected significantly by large variations of stream noise levels and spectra. The noise conditions were varied with on or off control of boundary-layer bleed upstream of the nozzle throats and by varying the test unit Reynolds number. By appropriate manipulation of these test variables, the nozzle-wall boundary layers could be either maintained partially laminar or caused to be fully turbulent over the same range of unit Reynolds number. The corresponding stream noise levels were then either extremely low, with no energy at high frequencies, or were much higher, approaching the levels in conventional tunnels, but with energy at much higher frequencies than in conventional tunnels.

The quantitative effects of these variable-noise conditions on the transition Reynolds numbers in the quiet tunnels are demonstrated in this report by correlations with previous data in several conventional wind tunnels and in flight where the local Mach number range was restricted to values between 1.5 and 5. Correlation parameters were developed for this purpose that utilize functions of the distance from the cone apex and of a wave number which characterizes the higher frequency energy found in the quiet-tunnel noise spectra. These functions were normalized so that when the external noise was spatially uniform and contained only low-frequency components, as measured in conventional wind tunnels and in flight, the root-mean-square noise parameters used in previous correlations of these data were recovered. However, when the functions were applied to the quiet-tunnel data for which large axial variations in noise levels and spectra occurred, they modified the local noise and appeared to account indirectly for variations in local receptivity of the cone boundary layer in response to the quiet-tunnel variable-noise conditions.

The final correlation results then showed that transition in these quiet tunnels was dominated by the local stream noise incident on the cone boundary layer upstream of the neutral stability point. The noise incident on the boundary layer downstream of the neutral stability point apparently had an exponentially decreasing effect on

transition as the distance from the neutral point increased. The correlation results also suggested that frequencies, or wave numbers, in the region of peak spectral energies may be involved directly in the transition process.

The extent of the transition region, expressed as the ratio of the flow distance to transition onset to the flow distance to transition end, correlates with essentially the same noise parameters used for the transition-onset Reynolds numbers. This ratio therefore correlates directly with the transition-onset Reynolds number for all the data used herein.

Langley Research Center
National Aeronautics and Space Administration
Hampton, VA 23665
November 18, 1983

REFERENCES

1. Pate, S. R.; and Schueler, C. J.: Radiated Aerodynamic Noise Effects on Boundary-Layer Transition in Supersonic and Hypersonic Wind Tunnels. AIAA J., vol. 7, no. 3, Mar. 1969, pp. 450-457.
2. Pate, S. R.: Measurements and Correlations of Transition Reynolds Numbers on Sharp Slender Cones at High Speeds. AIAA J., vol. 9, no. 6, June 1971, pp. 1082-1090. (Available from DTIC as AD 698 326.)
3. Laufer, John: Sound Radiation From a Turbulent Boundary Layer. The Mechanics of Turbulence, Gordon & Breach, Sci. Pub., Inc., c.1964, pp. 381-393.
4. Laufer, John: Some Statistical Properties of the Pressure Field Radiated by a Turbulent Boundary Layer. Phys. Fluids, vol. 7, no. 8, Aug. 1964, pp. 1191-1197.
5. Stainback, P. Calvin: Hypersonic Boundary-Layer Transition in the Presence of Wind-Tunnel Noise. AIAA J., vol. 9, no. 12, Dec. 1971, pp. 2475-2476.
6. Stainback, P. C.; Fischer, M. C.; and Wagner, R. D.: Effects of Wind-Tunnel Disturbances on Hypersonic Boundary-Layer Transition. Pts. I and II. AIAA Paper No. 72-181, Jan. 1972.
7. Fischer, M. C.; and Wagner, R. D.: Transition and Hot-Wire Measurements in Hypersonic Helium Flow. AIAA J., vol. 10, no. 10, Oct. 1972, pp. 1326-1332.
8. Pate, S. R.: Comparison of NASA Helium Tunnel Transition Data With Noise-Transition Correlation. AIAA J., vol. 12, no. 11, Nov. 1974, p. 1615.
9. Morkovin, Mark V.: Critical Evaluation of Transition From Laminar to Turbulent Shear Layers With Emphasis on Hypersonically Traveling Bodies. AFFDL-TR-68-149, U.S. Air Force, Mar. 1969. (Available from DTIC as AD 686 178.)
10. Reshotko, Eli: A Program for Transition Research. AIAA J., vol. 13, no. 3, Mar. 1975, pp. 261-265.
11. Reshotko, Eli: Boundary-Layer Stability and Transition. Annual Review of Fluid Mechanics, Volume 8, Milton Van Dyke, Walter G. Vincenti, and J. V. Wehausen, eds., Annual Rev., Inc., 1976, pp. 311-349.
12. Beckwith, Ivan E.; and Bertram, Mitchel H.: A Survey of NASA Langley Studies on High-Speed Transition and the Quiet Tunnel. NASA TM X-2566, 1972.
13. Beckwith, Ivan E.; Harvey, William D.; Harris, Julius E.; and Holley, Barbara B.: Control of Supersonic Wind-Tunnel Noise by Laminarization of Nozzle-Wall Boundary Layers. NASA TM X-2879, 1973.
14. Beckwith, I. E.: Development of a High Reynolds Number Quiet Tunnel for Transition Research. AIAA J., vol. 13, no. 3, Mar. 1975, pp. 300-306.
15. Beckwith, I. E.; Anders, J. B.; Stainback, P. C.; Harvey, W. D.; and Srokowski, A. J.: Progress in the Development of a Mach 5 Quiet Tunnel. Laminar-Turbulent Transition, AGARD-CP-224, Oct. 1977, pp. 28-1 - 28-14.

16. Anders, J. B.; Stainback, P. C.; and Beckwith, I. E.: New Technique for Reducing Test Section Noise in Supersonic Wind Tunnels. AIAA J., vol. 18, no. 1, Jan. 1980, pp. 5-6.
17. Creel, T. R.; and Beckwith, I. E.: Wind Tunnel Noise Reduction at Mach 5 With a Rod-Wall Sound Shield. AIAA J., vol. 21, no. 5, May 1983, pp. 643-644.
18. Beckwith, Ivan E.; and Moore, William O., III: Mean Flow and Noise Measurements in a Mach 3.5 Pilot Quiet Tunnel. A Collection of Technical Papers - AIAA 12th Aerodynamic Testing Conference, Mar. 1982, pp. 48-70. (Available as AIAA-82-0569.)
19. Beckwith, Ivan E.; Creel, Theodore R., Jr.; Chen, Fang-Jenq; and Kendall, James M.: Free-Stream Noise and Transition Measurements on a Cone in a Mach 3.5 Pilot Low-Disturbance Tunnel. NASA TP-2180, 1983.
20. Krogmann, P.: An Experimental Study of Boundary Layer Transition on a Slender Cone at Mach 5. Laminar-Turbulent Transition, AGARD-CP-224, Oct. 1977, pp. 26-1 - 26-12.
21. Potter, J. Leith: Boundary-Layer Transition on Supersonic Cones in an Aeroballistic Range. AIAA J., vol. 13, no. 3, Mar. 1975, pp. 270-277.
22. Morkovin, Mark V.: Technical Evaluation Report of the Fluid Dynamics Panel Symposium on Laminar-Turbulent Transition. AGARD-AR-122, June 1978.
23. Dougherty, N. S., Jr.; and Fisher, D. F.: Boundary-Layer Transition on a 10-Deg Cone: Wind Tunnel/Flight Correlation. AIAA-80-0154, Jan. 1980.
24. Dougherty, N. Sam, Jr.; and Fisher, David F.: Boundary-Layer Transition Correlation on a Slender Cone in Wind Tunnels and Flight Indications of Flow Quality. AEDC-TR-81-26, U.S. Air Force, Feb. 1982. (Available from DTIC as AD A111 328.)
25. Masaki, M.; and Yakura, J. K.: Transitional Boundary-Layer Considerations for the Heating Analyses of Lifting Re-Entry Vehicles. J. Spacecr., vol. 6, no. 9, Sept. 1969, pp. 1048-1053.
26. Harvey, W. D.; and Bobbitt, P. J.: Some Anomalies Between Wind Tunnel and Flight Transition Results. AIAA-81-1225, June 1981.
27. Mack, Leslie M.: Progress in Compressible Boundary Layer Stability Computations. Proceedings of the Boundary Layer Transition Workshop, Volume IV, TOR-0172(S2816-16)-5 (Contract No. F04701-71-C-0172), Aerosp. Corp., Dec. 20, 1971, pp. 1-1 - 1-19.
28. Kendall, James M., Jr.: JPL Experimental Investigations. Proceedings of the Boundary Layer Transition Workshop, Volume IV, TOR-0172(S2816-16)-5 (Contract No. F04701-71-C-0172), Aerosp. Corp., Dec. 20, 1971, pp. 2-1 - 2-16.
29. Mack, Leslie M.: A Numerical Method for the Prediction of High-Speed Boundary-Layer Transition Using Linear Theory. Aerodynamic Analyses Requiring Advanced Computers - Part I, NASA SP-347, 1975, pp. 101-123.

30. Mack, Leslie M.: Linear Stability Theory and the Problem of Supersonic Boundary-Layer Transition. AIAA J., vol. 13, no. 3, Mar. 1975, pp. 278-289.
31. Kendall, J. M.: Wind Tunnel Experiments Relating to Supersonic and Hypersonic Boundary-Layer Transition. AIAA J., vol. 13, no. 3, Mar. 1975, pp. 290-299.
32. Morkovin, Mark V.: Instability, Transition to Turbulence and Predictability. AGARD-AG-236, July 1978.
33. Trimpi, Robert L.: Modern Fluid Dynamics of Supersonic and Hypersonic Flight. AIAA-80-0862, May 1980.
34. Anders, J. B.; Stainback, P. C.; Keefe, L. R.; and Beckwith, I. E.: Fluctuating Disturbances in a Mach 5 Wind Tunnel. AIAA J., vol. 15, no. 8, Aug. 1977, pp. 1123-1129.
35. Anders, J. B.; Stainback, P. C.; and Beckwith, I. E.: A New Technique for Reducing Test Section Noise in Supersonic Wind Tunnels. A Collection of Technical Papers - AIAA 10th Aerodynamic Testing Conference, Apr. 1978, pp. 354-364. (Available as AIAA Paper 78-817.)
36. Beckwith, Ivan E.; and Holley, Barbara B.: Görtler Vortices and Transition in Wall Boundary Layers of Two Mach 5 Nozzles. NASA TP-1869, 1981.
37. Reda, Daniel C.: Boundary-Layer Transition Experiments on Sharp, Slender Cones in Supersonic Free Flight. AIAA J., vol. 17, no. 8, Aug. 1979, pp. 803-810.
38. Dougherty, N. Sam, Jr.: Influence of Wind Tunnel Noise on the Location of Boundary-Layer Transition on a Slender Cone at Mach Numbers From 0.2 to 5.5. U.S. Air Force, Mar. 1980.
Volume I - Experimental Methods and Summary of Results. AEDC-TR-78-44-VOL-1. (Available from DTIC as AD A083 165.)
Volume II - Tabulated and Plotted Data. AEDC-TR-78-44-VOL-2. (Available from DTIC as AD A083 166.)
39. Laufer, John; and Marte, Jack E.: Results and a Critical Discussion of Transition-Reynolds-Number Measurements on Insulated Cones and Flat Plates in Supersonic Wind Tunnels. Rep. No. 20-96 (Contract No. DA-04-495-Ord 18), Jet Propul. Lab., California Inst. Technol., Nov. 30, 1955.
40. Fisher, David F.; and Dougherty, N. Sam, Jr.: In-Flight Transition Measurement on a 10° Cone at Mach Numbers From 0.5 to 2.0. NASA TP-1971, 1982.
41. Strike, W. T., Jr.; Donaldson, J. C.; and Beale, D. K.: Test Section Turbulence in the AEDC/VKF Supersonic/Hypersonic Wind Tunnels. AEDC-TR-81-5, U.S. Air Force, July 1981. (Available from DTIC as AD A102 615.)
42. Laderman, A. J.: Review of Wind-Tunnel Freestream Pressure Fluctuations. AIAA J., vol. 15, no. 4, Apr. 1977, pp. 605-608.
43. Harvey, William D.: Influence of Free-Stream Disturbances on Boundary-Layer Transition. NASA TM-78635, 1978.

44. Malik, Mujeeb R.: COSAL - A Black-Box Compressible Stability Analysis Code for Transition Prediction in Three-Dimensional Boundary Layers. NASA CR-165925, 1982.
45. Reshotko, Eli: Stability Theory as a Guide to the Evaluation of Transition Data. AIAA J., vol. 7, no. 6, June 1969, pp. 1086-1091.
46. Dhawan, S.; and Narasimha, R.: Some Properties of Boundary Layer Flow During the Transition From Laminar to Turbulent Motion. J. Fluid Mech., vol. 3, pt. 4, Jan. 1958, pp. 418-436.
47. Spangenberg, W. G.; and Rowland, W. R.: Optical Study of Boundary-Layer Transition Processes in a Supersonic Air Stream. Phys. Fluids, vol. 3, no. 5, Sept.-Oct. 1960, pp. 667-684.
48. Chen, Karl K.; and Thyson, Noel A.: Extension of Emmons' Spot Theory to Flows on Blunt Bodies. AIAA J., vol. 9, no. 5, May 1971, pp. 821-825.
49. Pate, Samuel R.: Effects of Wind Tunnel Disturbances on Boundary-Layer Transition With Emphasis on Radiated Noise: A Review. AIAA-80-0431, Mar. 1980.

TABLE I.- SELECTED TRANSITION DATA FROM TWO QUIET-TUNNEL INVESTIGATIONS

(a) $M_\infty = 3.5$; data taken from reference 19

$R_\infty/\text{in.}$	$R_e/\text{in.}$	Neutral-point $s_N, \text{in.}$	Bleed valve open				Bleed valve closed			
			$x_{\text{tip}} = 5 \text{ in.}$		$x_{\text{tip}} = 8 \text{ in.}$		$x_{\text{tip}} = 5 \text{ in.}$		$x_{\text{tip}} = 8 \text{ in.}$	
			$R_{e,T}$	s_T/s_{TE}	$R_{e,T}$	s_T/s_{TE}	$R_{e,T}$	s_T/s_{TE}	$R_{e,T}$	s_T/s_{TE}
2.5×10^5	2.7×10^5	2.4					3.3×10^6	0.84	2.4×10^6	0.80
5.3	5.7	1.3	7.0×10^6	0.91	5.2×10^6	0.88	3.0	.70	2.0	.63
7.9	8.5	.9	8.0	.89	5.8	.87	3.8	.78	3.4	.75
10.0	10.8	.8	4.8	.78	3.4	.72	4.0	.76	3.4	.73
12.6	13.6	.7	4.1	.73	3.4	.67	4.0	.74	3.3	.68
14.8	16.0	.6	3.2	.60	3.2	.65	3.5	.69	3.5	.66

(b) $M_\infty = 5.0$; data taken by Schopper

$x_{\text{tip}}, \text{in.}$	$R_\infty/\text{in.}$	$R_e/\text{in.}$	$R_{\infty,TE}$	$R_{e,TE}$	$R_{e,T}$	s_T/s_{TE}
Bleed valve open						
5.7	6.9×10^5	7.9×10^5	5.4×10^6	6.2×10^6	5.3×10^6	0.86
	11.4	13.1	4.1	4.7	3.4	.72
7.6	6.1×10^5	7.0×10^5	4.5×10^6	5.2×10^6	4.0×10^6	0.78
	9.4	10.8	3.0	3.4	2.3	.68
Bleed valve closed						
5.7	5.6×10^5	6.4×10^5	4.4×10^6	5.1×10^6	3.9×10^6	0.77
	7.0	8.0	5.0	5.7	4.7	.82
	8.4	9.6	4.3	4.9	3.7	.75
	11.6	13.3	4.8	5.6	4.5	.81
7.6	4.4×10^5	5.1×10^5	3.6×10^6	4.1×10^6	2.9×10^6	0.70
	7.0	8.0	3.6	4.2	2.9	.70
	10.2	11.7	3.1	3.6	2.5	.69

TABLE II.- VARIATION OF ROOT-MEAN-SQUARE NOISE AND FREQUENCY
AT SPECTRAL PEAK FOR MACH 3.5 QUIET TUNNEL

(a) Bleed valve open

$R_{\infty} = 5.3 \times 10^5$ per inch				$R_{\infty} = 7.9 \times 10^5$ per inch			
X, in.	\tilde{p}/\bar{q} , percent	f_m , kHz	$F_m \times 10^5$	X, in.	\tilde{p}/\bar{q} , percent	f_m , kHz	$F_m \times 10^5$
4.5	0.003	3	0.13	4.5	0.006	2	0.06
5.5	.003	1	.04	5.5	.001	1	.03
6.5	.002	2	.09	6.5	.005	6	.18
7.5	.003	1	.04	7.5	.001	8	.24
8.5	.003	3	.13	8.5	.003	15	.45
9.5	.009	5	.22	9.5	.006	25	.75
10.5	.008	8	.36	10.5	.023	35	1.05
11.5	.022	9	.40	11.5	.033	45	1.35
12.5	.046	15	.67	12.5	.032	44	1.32
13.5	.045	21	.94	13.5	.026	30	.90
14.5	.042	20	.90	14.5	.029	18	.54
15.5	.048	26	1.16	15.5	.038	14	.42
16.5	.048	21	.94	16.5	.042	13	.39
17.5	.050	20	.90	17.5	.047	18	.54
18.5	.055	28	1.25	18.5	.049	17	.51
19.5	.060	16	.72	19.5	.051	14	.42
20.5	.067	21	.94	20.5	.055	15	.45
21.5	.065	23	1.03	21.5	.055	12	.36
22.5	.067	21	.94	22.5	.058	12	.36
23.5	.067	24	1.08	23.5	.056	22	.66
24.5	.075	15	.67	24.5	.063	14	.42

$R_{\infty} = 10.0 \times 10^5$ per inch				$R_{\infty} = 12.6 \times 10^5$ per inch			
X, in.	\tilde{p}/\bar{q} , percent	f_m , kHz	$F_m \times 10^5$	X, in.	\tilde{p}/\bar{q} , percent	f_m , kHz	$F_m \times 10^5$
4.5	0.003	30	0.71	4.5	0.006	32	0.60
5.5	.005	30	.71	5.5	.014	32	.60
6.5	.009	32	.76	6.5	.017	42	.79
7.5	.013	28	.66	7.5	.019	38	.72
8.5	.016	27	.64	8.5	.027	31	.58
9.5	.035	30	.71	9.5	.044	26	.49
10.5	.053	30	.71	10.5	.039	32	.60
11.5	.050	32	.76	11.5	.033	35	.66
12.5	.041	32	.76	12.5	.032	32	.60
13.5	.032	28	.66	13.5	.026	20	.38
14.5	.033	20	.47	14.5	.029		
15.5	.038	18	.43	15.5	.039		
16.5	.049	9	.21	16.5	.036	15	.28
17.5	.047			17.5	.037		
18.5	.051			18.5	.041		
19.5	.048			19.5	.039		
20.5	.053	12	.28	20.5	.044	14	.26
21.5	.052			21.5	.044		
22.5	.057			22.5	.048		
23.5	.056			23.5	.047		
24.5	.059	10	.24	24.5	.051	11	.21

TABLE II.- Continued

(a) Concluded

x, in.	$R_{\infty} = 14.8 \times 10^5$ per inch		
	\bar{p}/\bar{q} , percent	f_m , kHz	$F_m \times 10^5$
4.5	0.006	15	0.24
5.5	.011	20	.32
6.5	.016	35	.56
7.5	.020	25	.40
8.5	.029	18	.29
9.5	.041	20	.32
10.5	.034	18	.29
11.5	.029	18	.29
12.5	.027		
13.5	.025		
14.5	.027		
15.5	.027		
16.5	.035	14	.22
17.5	.035		
18.5	.038		
19.5	.038		
20.5	.043	13	.21
21.5	.043		
22.5	.048		
23.5	.047		
24.5	.053	16	.26

TABLE II.- Continued

(b) Bleed valve closed

$R_{\infty} = 2.5 \times 10^5$ per inch				$R_{\infty} = 5.3 \times 10^5$ per inch			
X, in.	\tilde{p}/\bar{q} , percent	f_m , kHz	$F_m \times 10^5$	X, in.	\tilde{p}/\bar{q} , percent	f_m , kHz	$F_m \times 10^5$
4.5	0.004	5	0.47	4.5	0.010	16	0.72
5.5	.009	5	.47	5.5	.044	20	.90
6.5	.003	5	.47	6.5	.067	22	.99
7.5	.007	5	.47	7.5	.073	22	.99
8.5	.022	7	.66	8.5	.067	22	.99
9.5	.058	9	.85	9.5	.049	20	.90
10.5	.074	10	.95	10.5	.038	20	.90
11.5	.071	9	.85	11.5	.035	21	.94
12.5	.070	9	.85	12.5	.037	20	.90
13.5	.057	8	.76	13.5	.034	14	.63
14.5	.055	9	.85	14.5	.036	13	.58
15.5	.060	7	.66	15.5	.043	13	.58
16.5	.075	9	.85	16.5	.056	11	.49
17.5	.070	10	.95	17.5	.053	22	.99
18.5	.069	8	.76	18.5	.058	20	.90
19.5	.069	10	.95	19.5	.062	22	.99
20.5	.076	13	1.23	20.5	.065	18	.81
21.5	.077	10	.95	21.5	.070	19	.85
22.5	.080	9	.85	22.5	.075	21	.94
23.5	.078	12	1.14	23.5	.073	20	.90
24.5	.089	8	.76	24.5	.082	19	.85

$R_{\infty} = 7.9 \times 10^5$ per inch				$R_{\infty} = 10.0 \times 10^5$ per inch			
X, in.	\tilde{p}/\bar{q} , percent	f_m , kHz	$F_m \times 10^5$	X, in.	\tilde{p}/\bar{q} , percent	f_m , kHz	$F_m \times 10^5$
4.5	0.009	60	1.80	4.5	0.009	75	1.78
5.5	.016	60	1.80	5.5	.015	70	1.66
6.5	.018	50	1.50	6.5	.016	70	1.66
7.5	.019	38	1.14	7.5	.017	30	.71
8.5	.021	35	1.05	8.5	.020	30	.71
9.5	.022	35	1.05	9.5	.021	30	.71
10.5	.023	30	.90	10.5	.020	32	.76
11.5	.025	30	.90	11.5	.023	30	.71
12.5	.028	30	.90	12.5	.026	30	.71
13.5	.024	25	.75	13.5	.023	25	.59
14.5	.028	20	.60	14.5	.030	30	.71
15.5	.035	15	.45	15.5	.032	18	.43
16.5	.046	16	.48	16.5	.038	19	.45
17.5	.048	18	.54	17.5	.039		
18.5	.051	18	.54	18.5	.043		
19.5	.064	12	.36	19.5	.049		
20.5	.063	13	.39	20.5	.056	15	.36
21.5	.062	12	.36	21.5	.056		
22.5	.066	13	.39	22.5	.060		
23.5	.066	12	.36	23.5	.060		
24.5	.075	12	.36	24.5	.067	12	.28

TABLE II.- Concluded

(b) Concluded

$R_{\infty} = 12.6 \times 10^5$ per inch				$R_{\infty} = 14.8 \times 10^5$ per inch			
X, in.	\tilde{p}/\bar{q} , percent	f_m , kHz	$F_m \times 10^5$	X, in.	\tilde{p}/\bar{q} , percent	f_m , kHz	$F_m \times 10^5$
4.5	0.010	72	1.36	4.5	0.010	66	1.06
5.5	.014	72	1.36	5.5	.013	65	1.04
6.5	.018	50	.94	6.5	.015	65	1.04
7.5	.016	50	.94	7.5	.015	45	.72
8.5	.018	50	.94	8.5	.015	40	.64
9.5	.022	45	.85	9.5	.017	25	.40
10.5	.022	30	.57	10.5	.017	28	.45
11.5	.021	25	.47	11.5	.017	25	.40
12.5	.023	32	.60	12.5	.023	19	.30
13.5	.022	24	.45	13.5	.019	20	.32
14.5	.023	17	.32	14.5	.022	21	.34
15.5	.030	6	.11	15.5	.034	11	.18
16.5	.039	8	.15	16.5	.038	15	.24
17.5	.041			17.5	.039		
18.5	.047			18.5	.042		
19.5	.046			19.5	.046		
20.5	.051	6	.11	20.5	.051	20	.32
21.5	.060			21.5	.051		
22.5	.067			22.5	.055		
23.5	.053			23.5	.053		
24.5	.063	5	.09	24.5	.061	11	.18

TABLE III.- DIMENSIONLESS FREQUENCY AT SPECTRAL PEAK OF STREAM
DISTURBANCES IN CONVENTIONAL TUNNELS AND FLIGHT

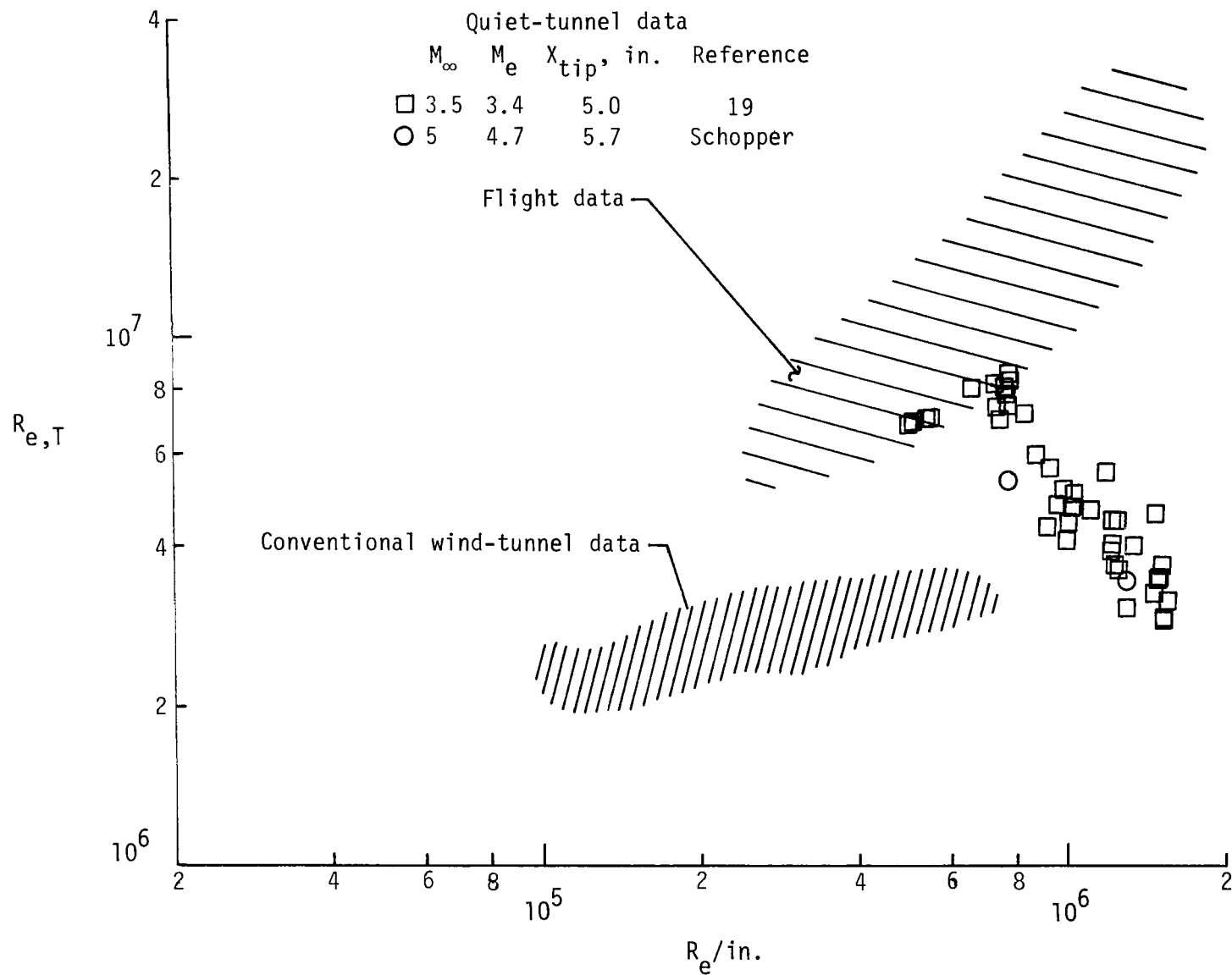
Source	M_∞	$R_\infty/\text{in.}$	F_m	$F_m/R_\infty/\text{in.}$	Probe	Reference
F-15 flight	1.35	2.4×10^5	1.1×10^{-6}	0.26	Pitot	40
AEDC Tunnel A	4.0	2.5	.93	.23	Hot wire	41
JPL 20-inch	2.0	3.4	.79	.27		4
	4.5	3.4	.74	.25		4
	3.3	.5	4.8	.24		19
	3.3	1.0	2.4	.24		19
	3.3	2.0	1.3	.26		19

TABLE IV.- SOURCE OF DATA AND CONDITIONS FOR CORRELATION FIGURES

[Used in figures 3 to 5 and 7 to 10]

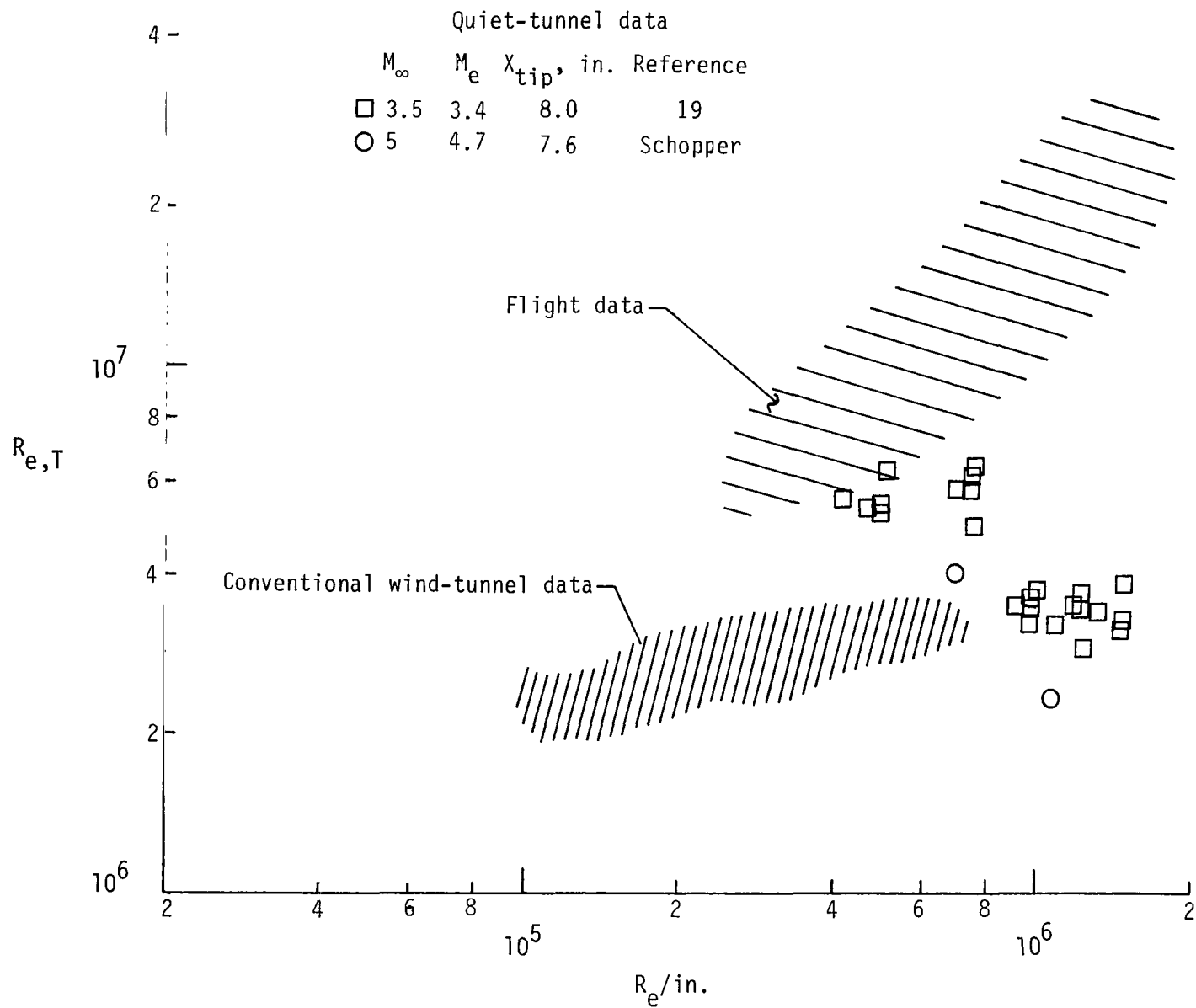
Symbol	$R_\infty/\text{in.}$	M_∞	M_e	Reference	Source
□	5.3 to 14.8×10^5	3.5	3.4	19	PQ tunnel with 2-D nozzle at LRC (B.V. open)
▣	2.5 to 14.8	3.5	3.4	19	PQ tunnel with 2-D nozzle at LRC (B.V. closed)
○	6.1 to 11.4	5	4.7	Schopper	PQ tunnel with axisymmetric nozzle at LRC (B.V. open)
⊕	^a 4.4 to 11.6	5	4.7	Schopper	PQ tunnel with axisymmetric nozzle at LRC (B.V. closed)
◇	2.0 to 2.4	1.6 to 2.0	1.5 to 1.9	38	Langley 4-Foot Supersonic Pressure Tunnel
△	2.1 to 4.1	2.9	2.8	38	Langley Unitary Plan Wind Tunnel (T.S. No. 1)
▽	1.7 to 4.3	2.9 to 3.5	2.8 to 3.4	38	Langley Unitary Plan Wind Tunnel (T.S. No. 2)
◇	1.7 to 10.0	6.0	5	5, 6	Langley 20-Inch Hypersonic Tunnel
▽	5.1 to 16.2	6.0	5	5, 6	Mach 6 high Reynolds number tunnel at LRC
△	1.9 to 2.9	1.6 to 2.5	1.6 to 2.4	38	Ames 9- by 7-Foot Supersonic Tunnel
◇	1.6 to 5.4	2.9 to 4.1	2.8 to 3.9	38	AEDC Tunnel A
◇	3.4	1.8 to 4.5	1.8 to 4.4	39	JPL 20-Inch Supersonic Tunnel
⬠	2.9 to 3.6	1.6 to 1.8	1.5 to 1.8	40	5° half-angle cone on F-15 airplane

^aIn figures 8(c) and 9, $R_\infty = 7.0 \times 10^5$ per inch.



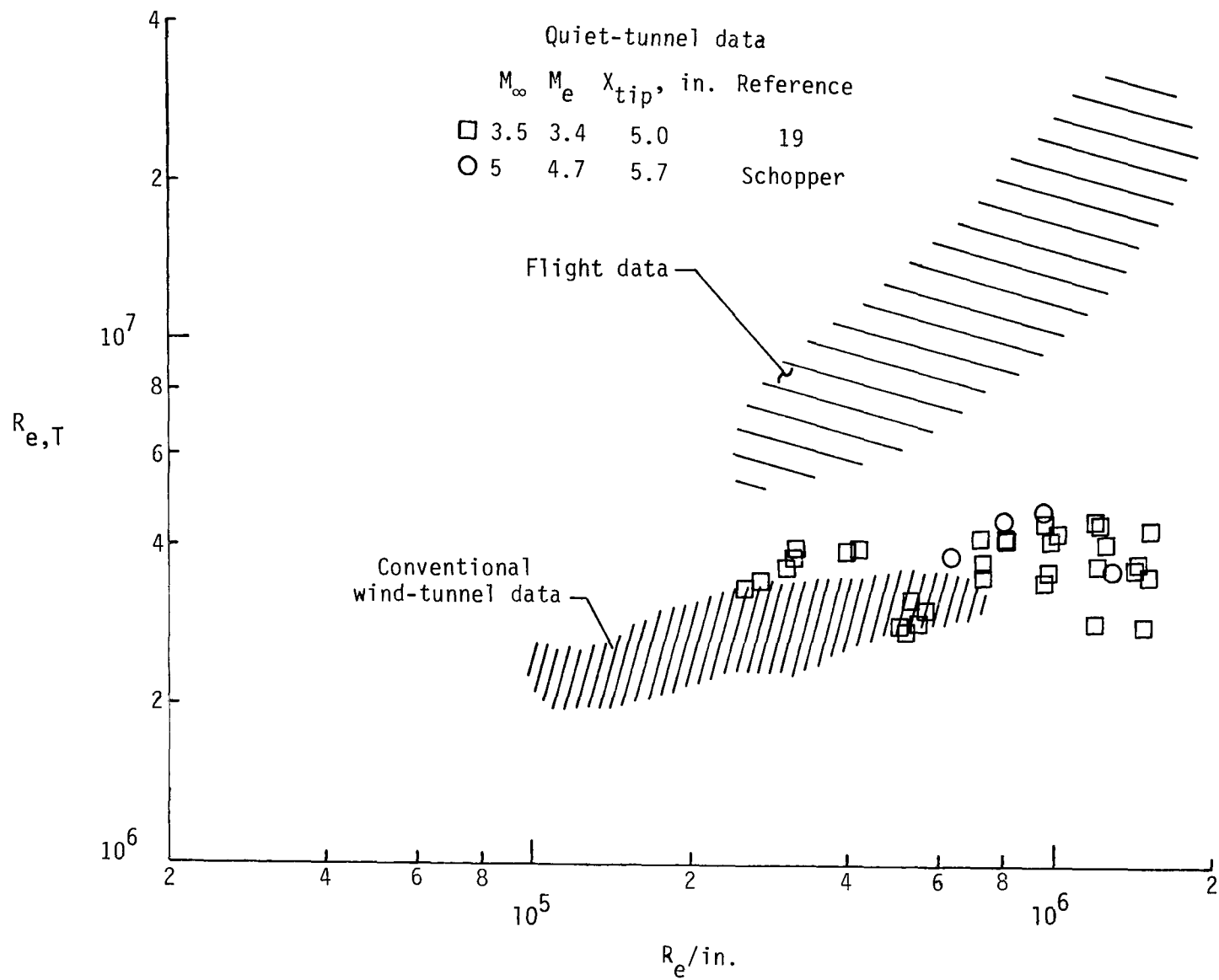
(a) Bleed valve open; cones in upstream location.

Figure 1.- Variation of $R_{e,T}$ with R_e on sharp-tip, 5° half-angle cones in two quiet tunnels compared with previous flight and wind-tunnel data.



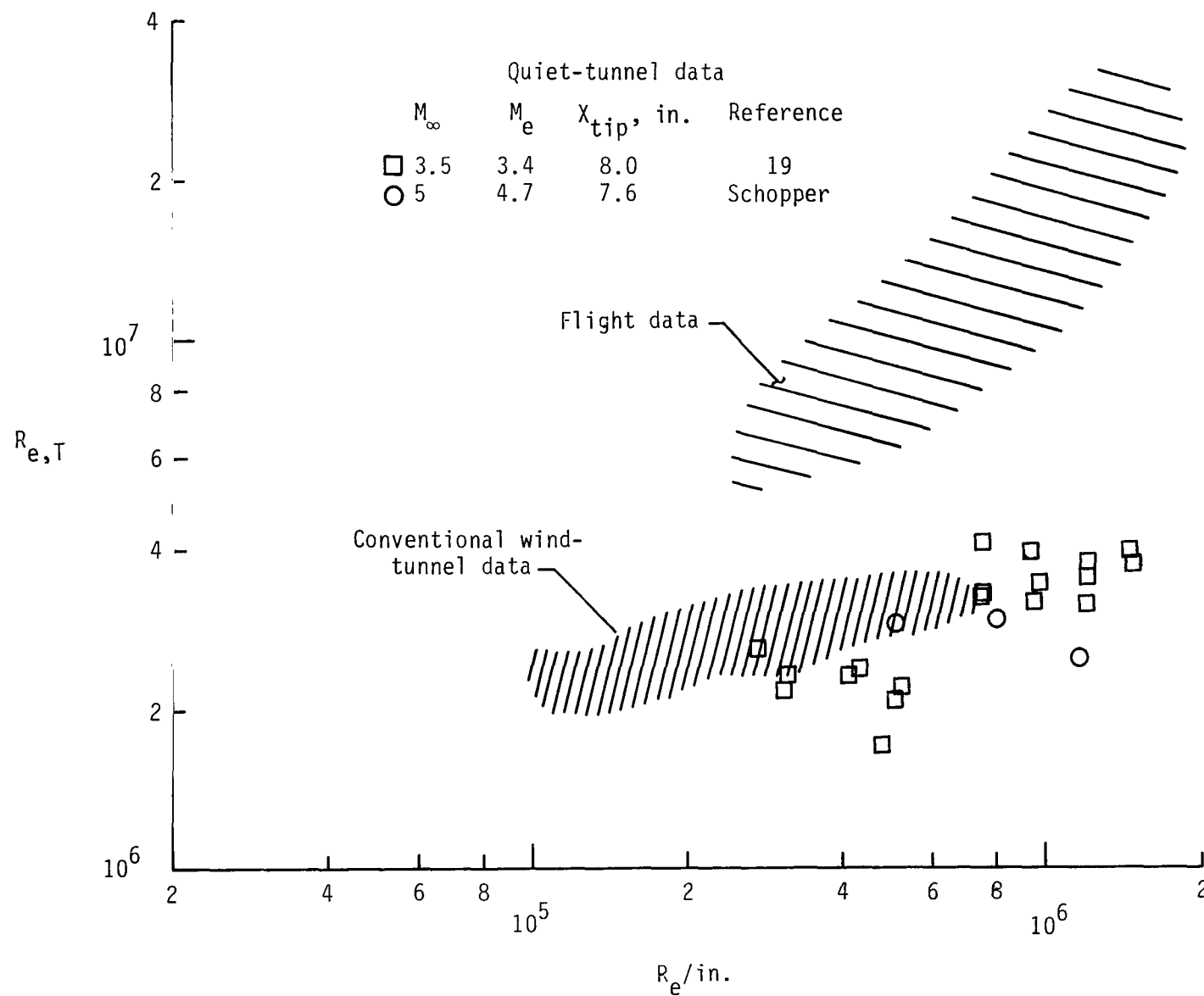
(b) Bleed valve open; cones in downstream location.

Figure 1.- Continued.



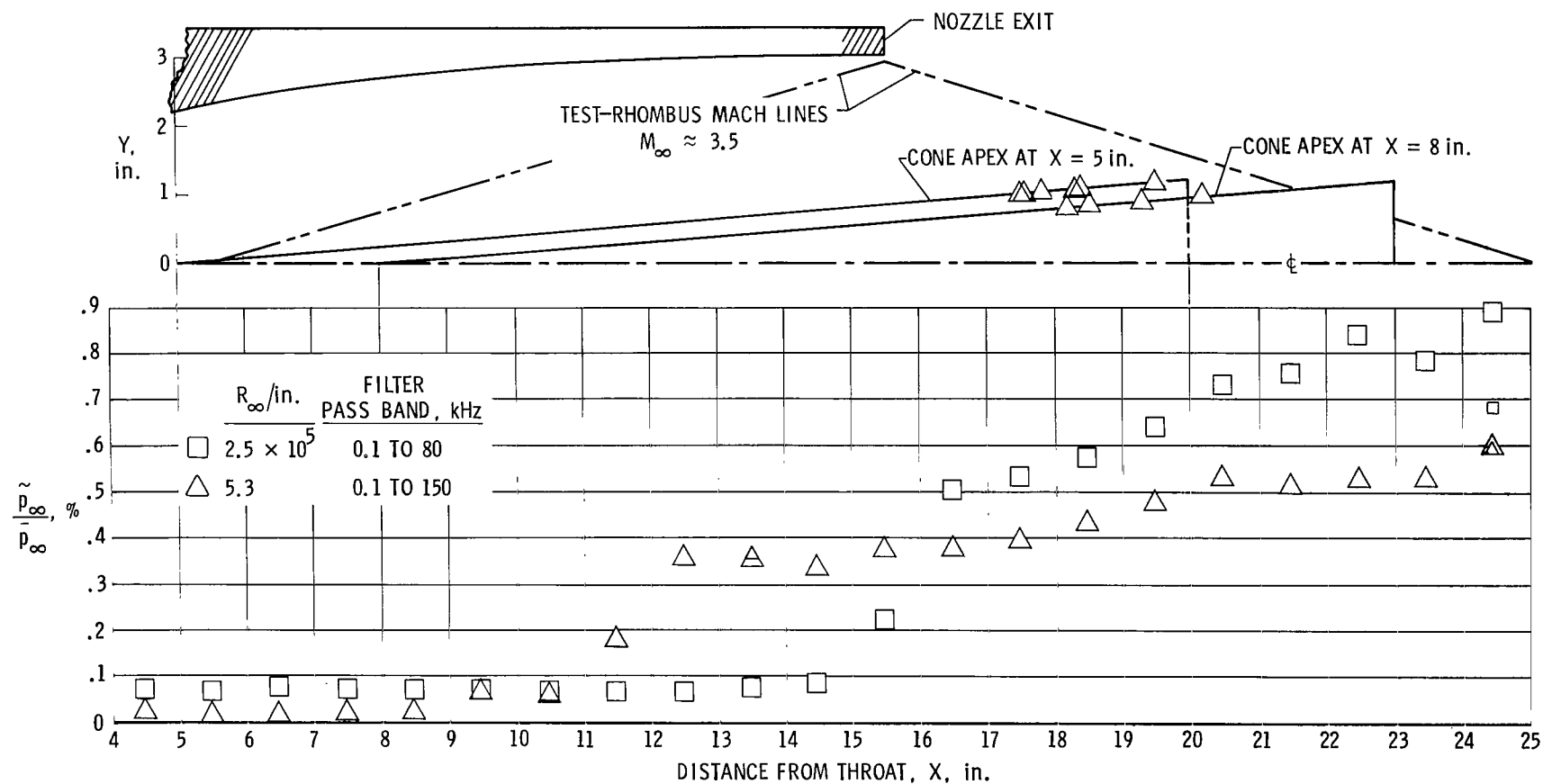
(c) Bleed valve closed; cones in upstream location.

Figure 1.- Continued.



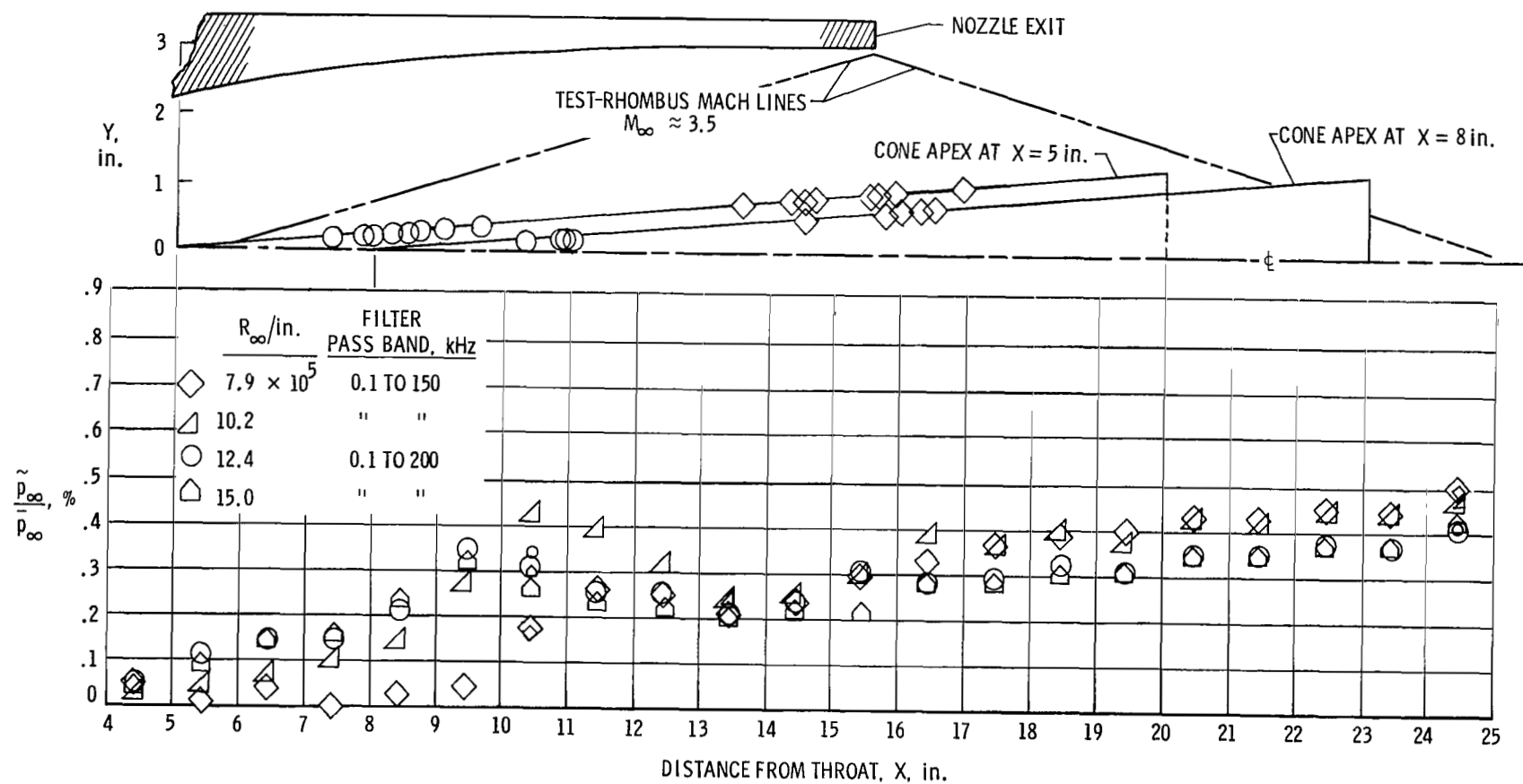
(d) Bleed valve closed; cones in downstream location.

Figure 1.- Concluded.



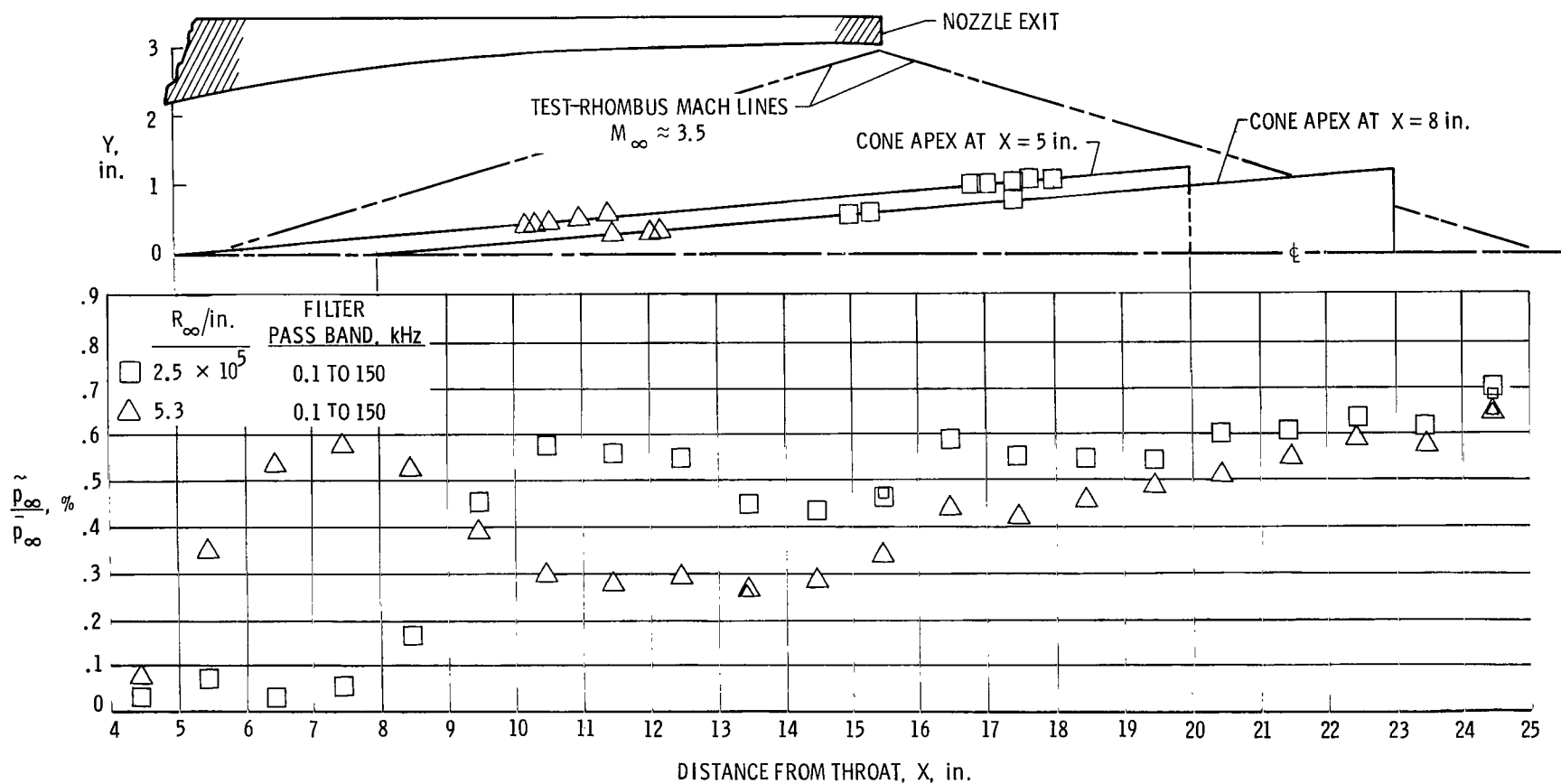
(a) $R_\infty \approx 2.5 \times 10^5$ and 5.3×10^5 per inch; bleed valve open.

Figure 2.- Variation along centerline of normalized rms static pressure from hot-wire measurements. Upper part of figure shows locations of transition X_T on cone in its two test positions for approximately the same unit Reynolds numbers denoted by the corresponding symbol used for rms pressure data.



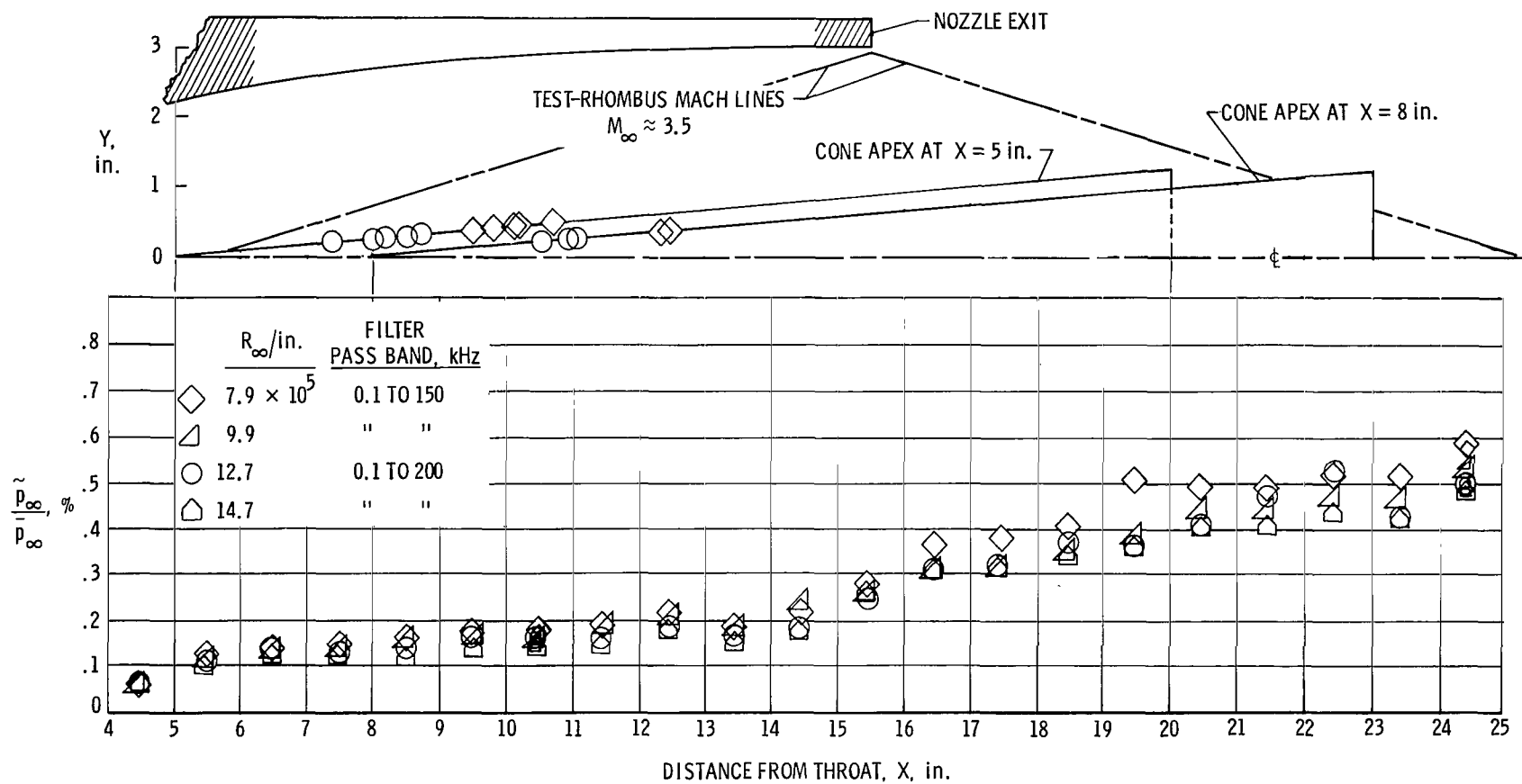
(b) $R_{\infty} \approx 7.9 \times 10^5$ to 15.0×10^5 per inch; bleed valve open.

Figure 2.- Continued.



(c) $R_{\infty} \approx 2.5 \times 10^5$ and 5.3×10^5 per inch; bleed valve closed.

Figure 2.- Continued.



(d) $R_{\infty} \approx 7.9 \times 10^5$ to 14.7×10^5 per inch; bleed valve closed.

Figure 2.- Concluded.

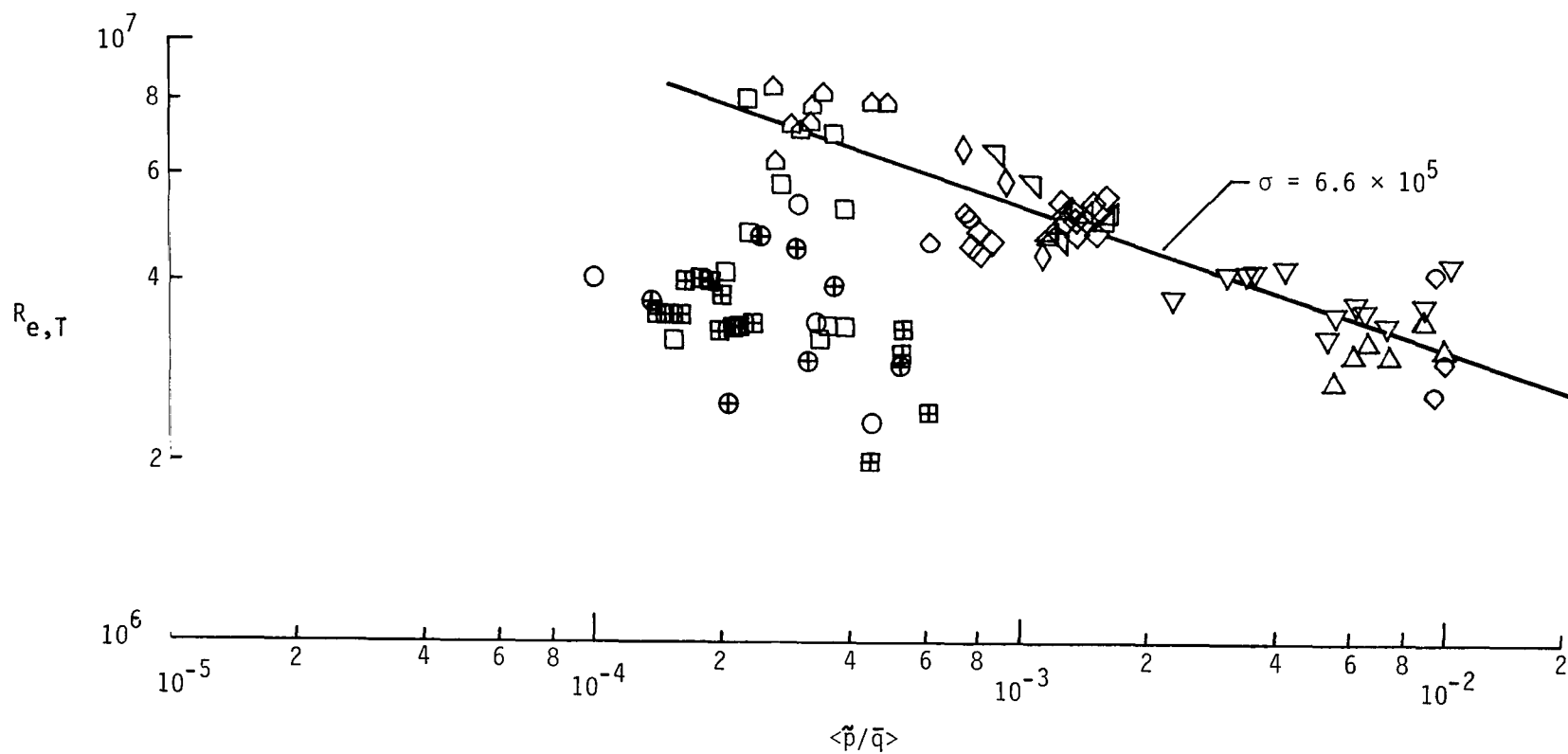
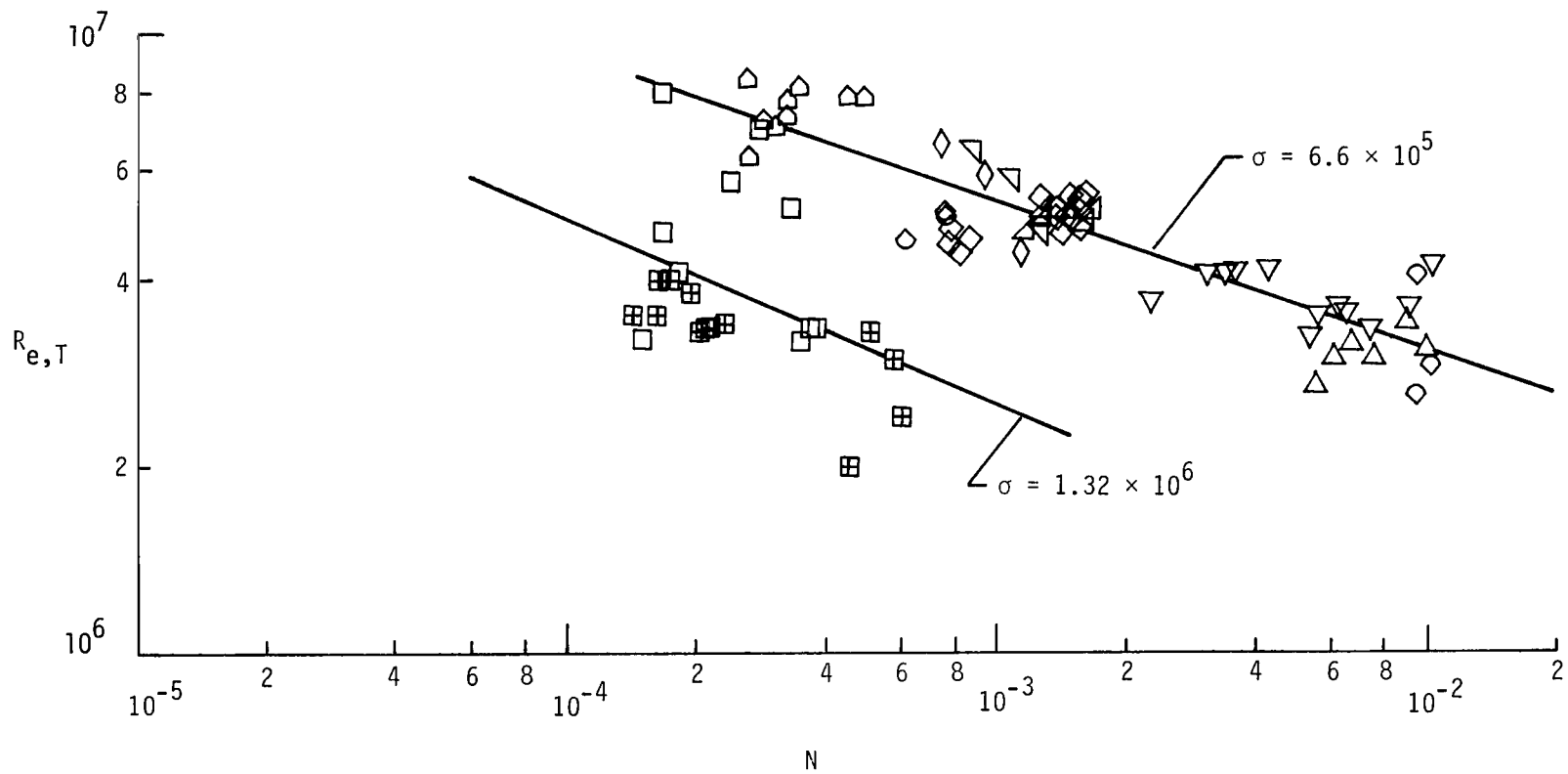
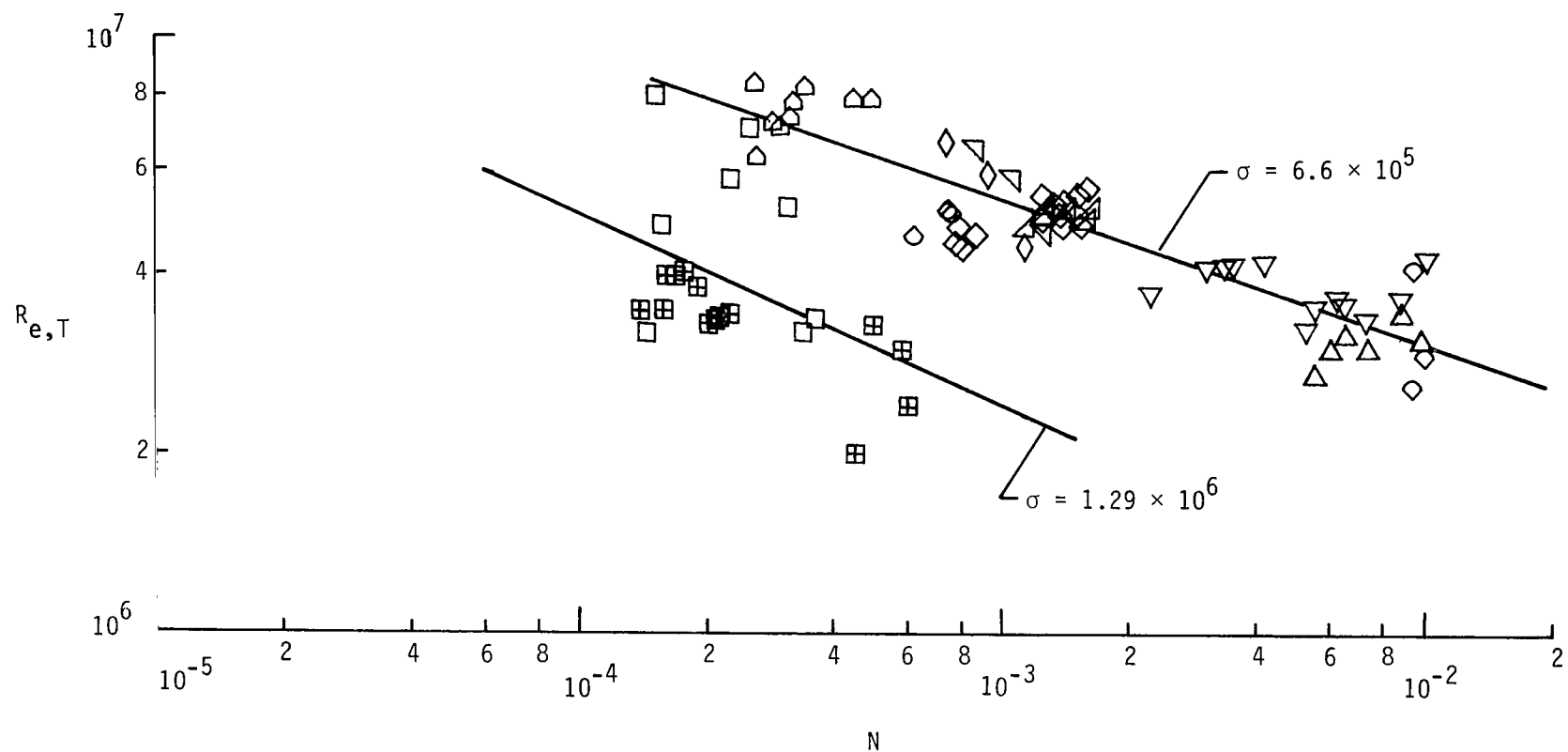


Figure 3.- Variation of $R_{e,T}$ with $\langle \tilde{p}/\bar{q} \rangle$ defined by equation (2). The solid line denotes a least-squares fit of conventional wind-tunnel and flight data. The symbols, flow conditions, and sources of the data used in this figure and in the remaining correlation figures are given in table IV.



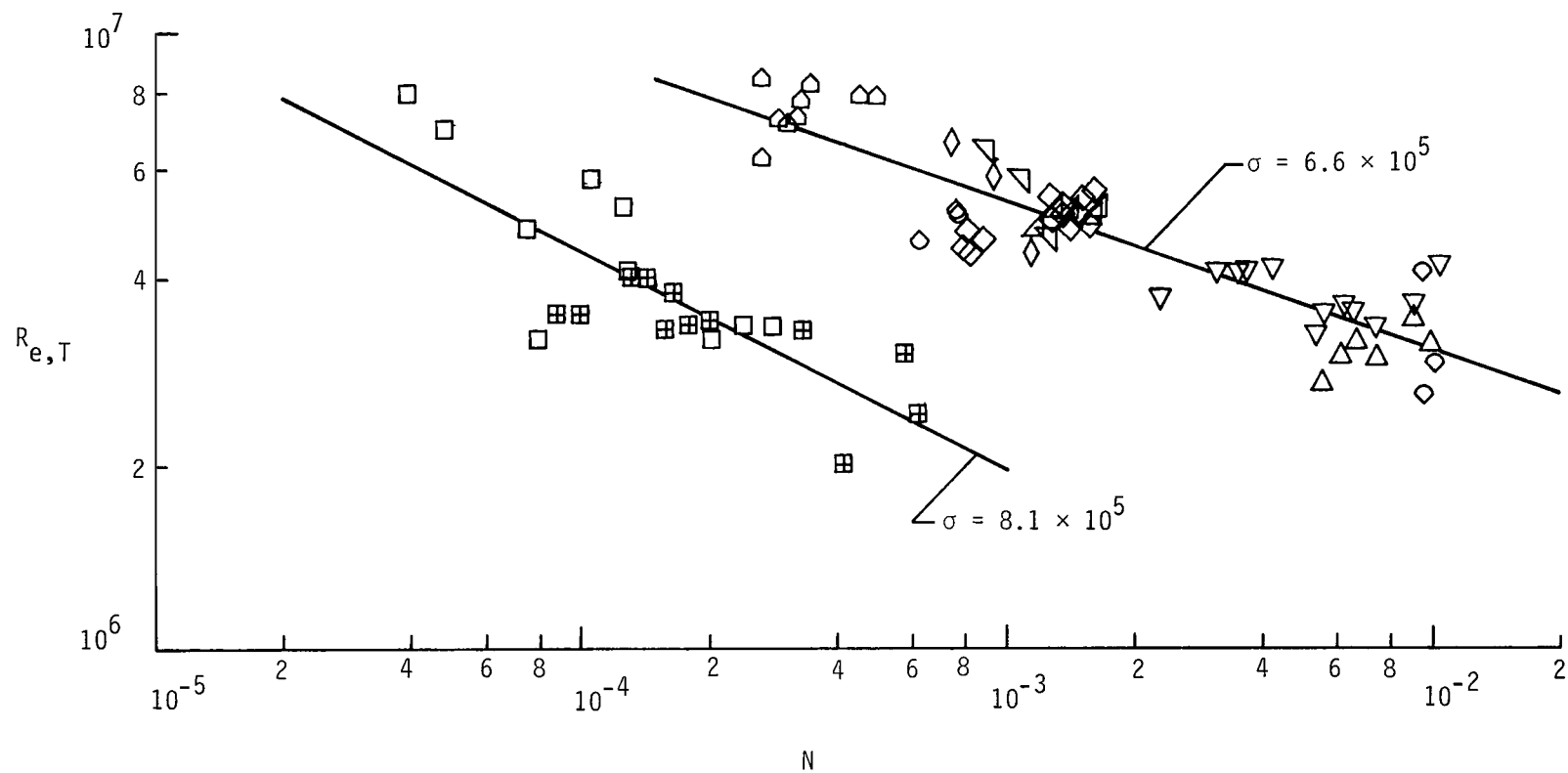
(a) With cosine function $A'P = \frac{\pi}{2} \cos\left(\frac{\pi}{2} \frac{s - s_N}{s_T - s_N}\right)$.

Figure 4.- Comparison between self-correlation of Mach 3.5 quiet-tunnel data and other data with different functions of $A'P$. Data symbols are defined in table IV.



(b) With linear function $A'P = 2 \frac{s - s_N}{s_T - s_N}$.

Figure 4.- Continued.



(c) With exponential function $A'P = 12 \exp\left(-12 \frac{s - s_N}{s_T - s_N}\right)$.

Figure 4.- Concluded.

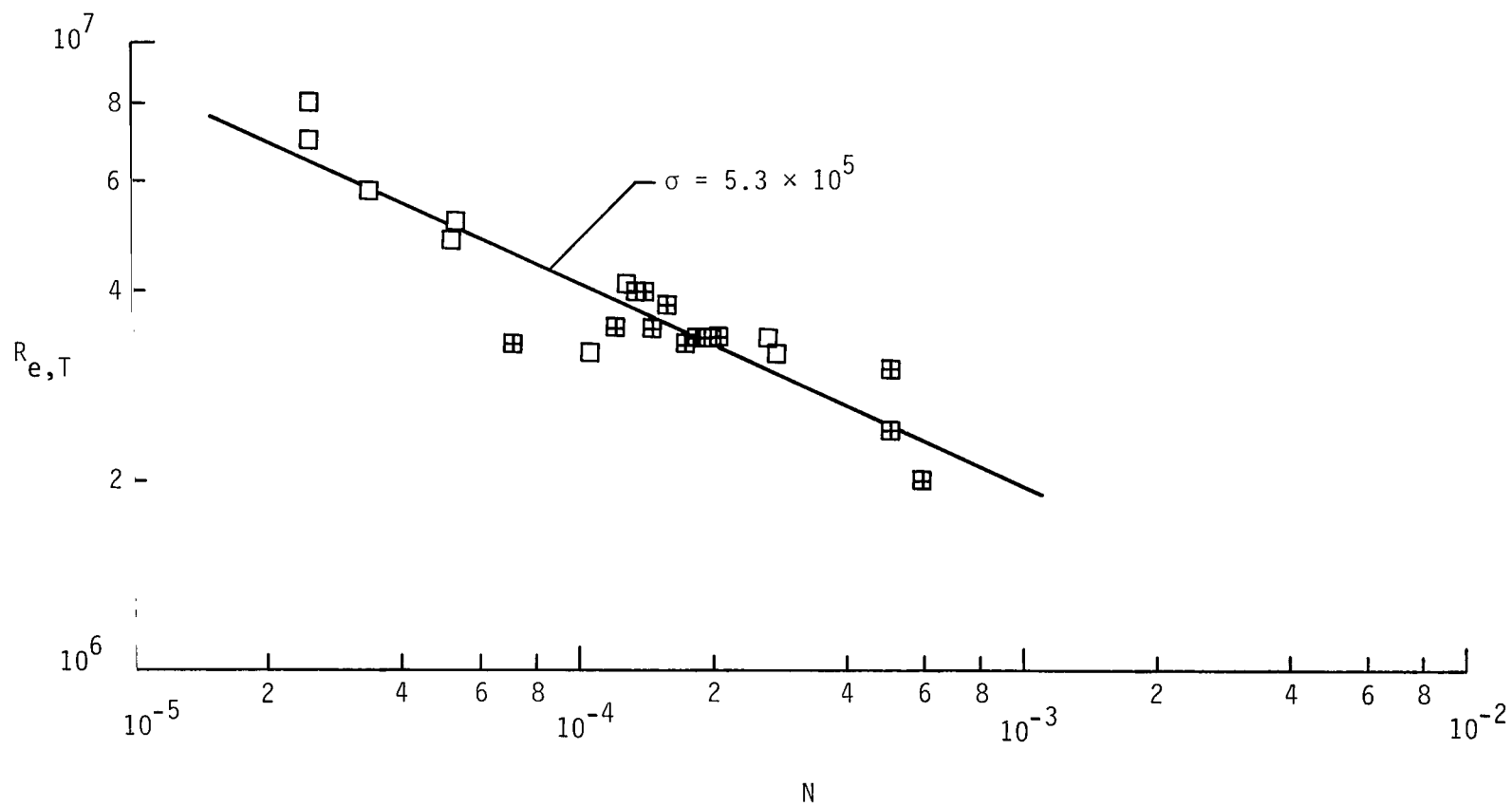
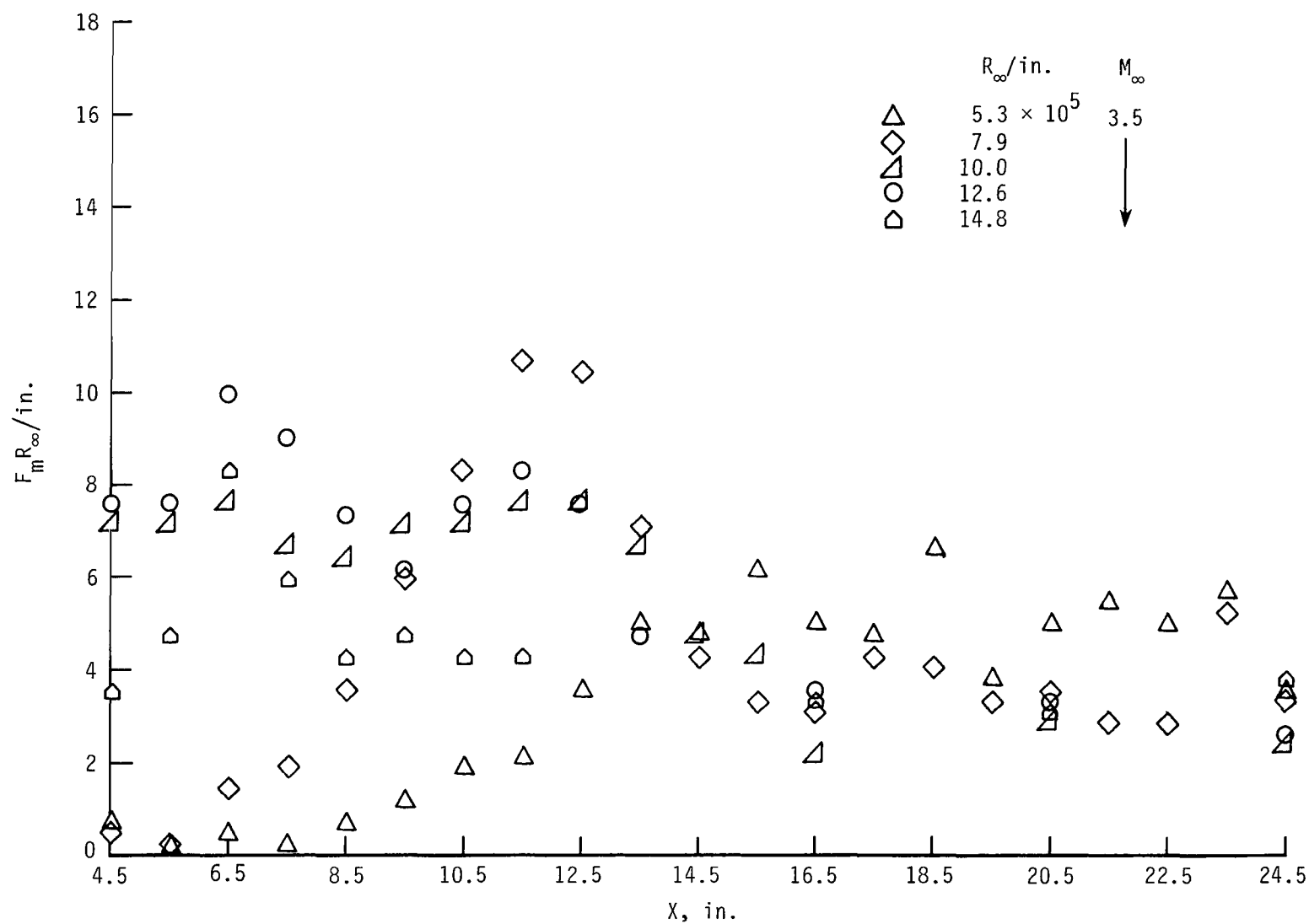


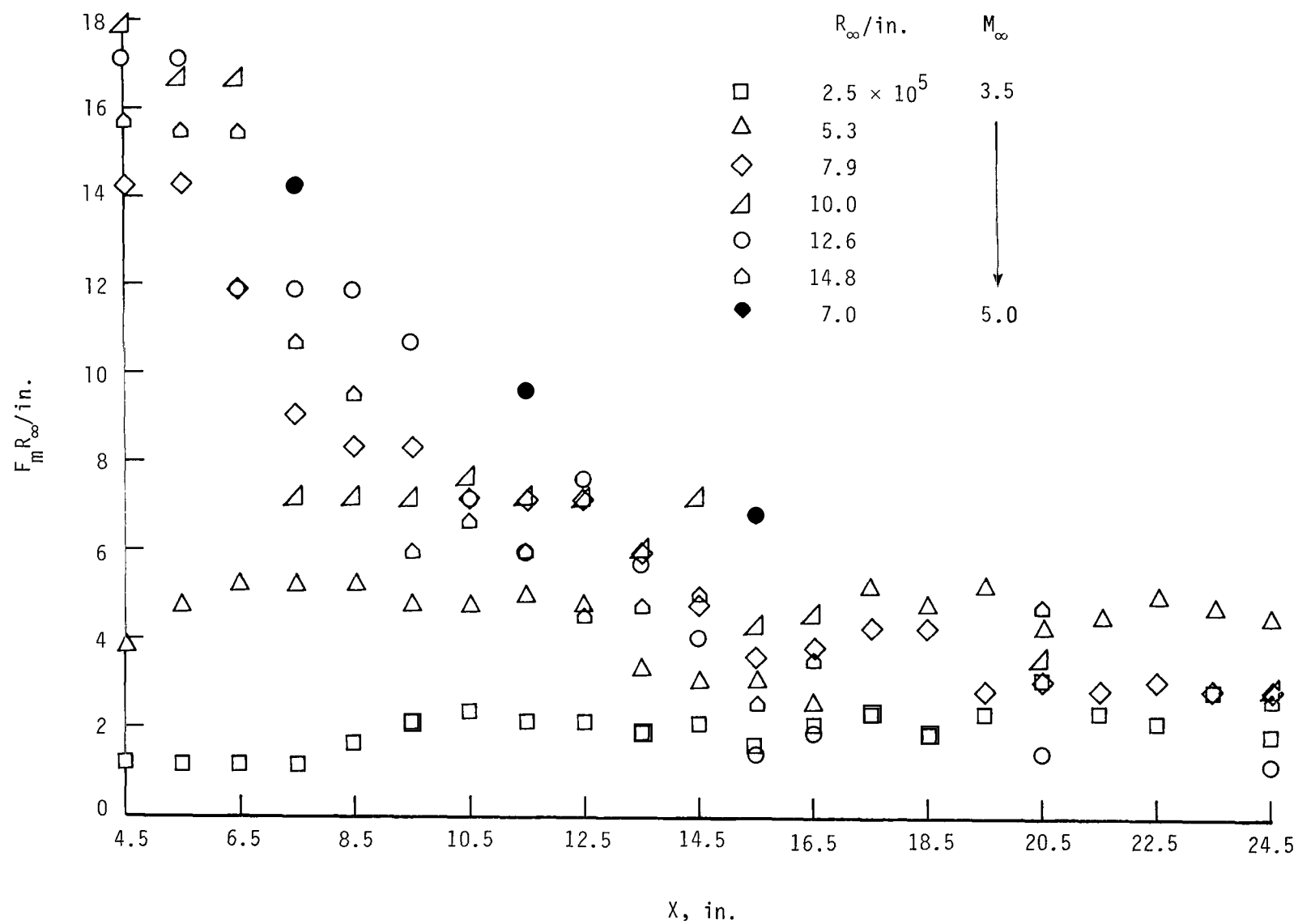
Figure 5.- Self-correlation of Mach 3.5 quiet-tunnel data with $N = \frac{1}{s_N} \int_0^{s_N} \frac{\tilde{p}}{q} ds$.

Data symbols are defined in table IV.



(a) Bleed valve open.

Figure 6.- Variation of $F_m R_\infty$ with X along nozzle axis in two quiet tunnels.



(b) Bleed valve closed.

Figure 6.- Concluded.

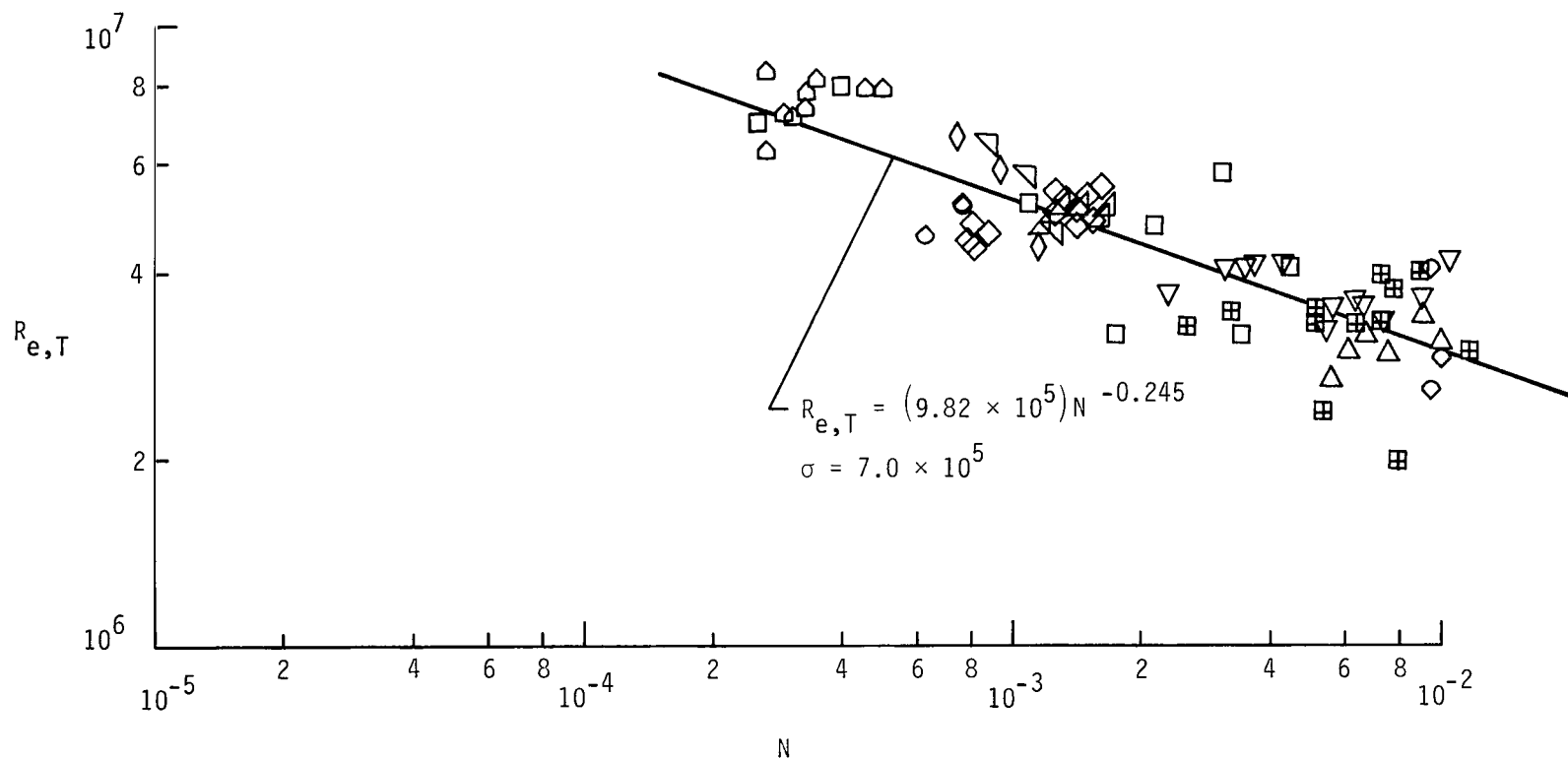
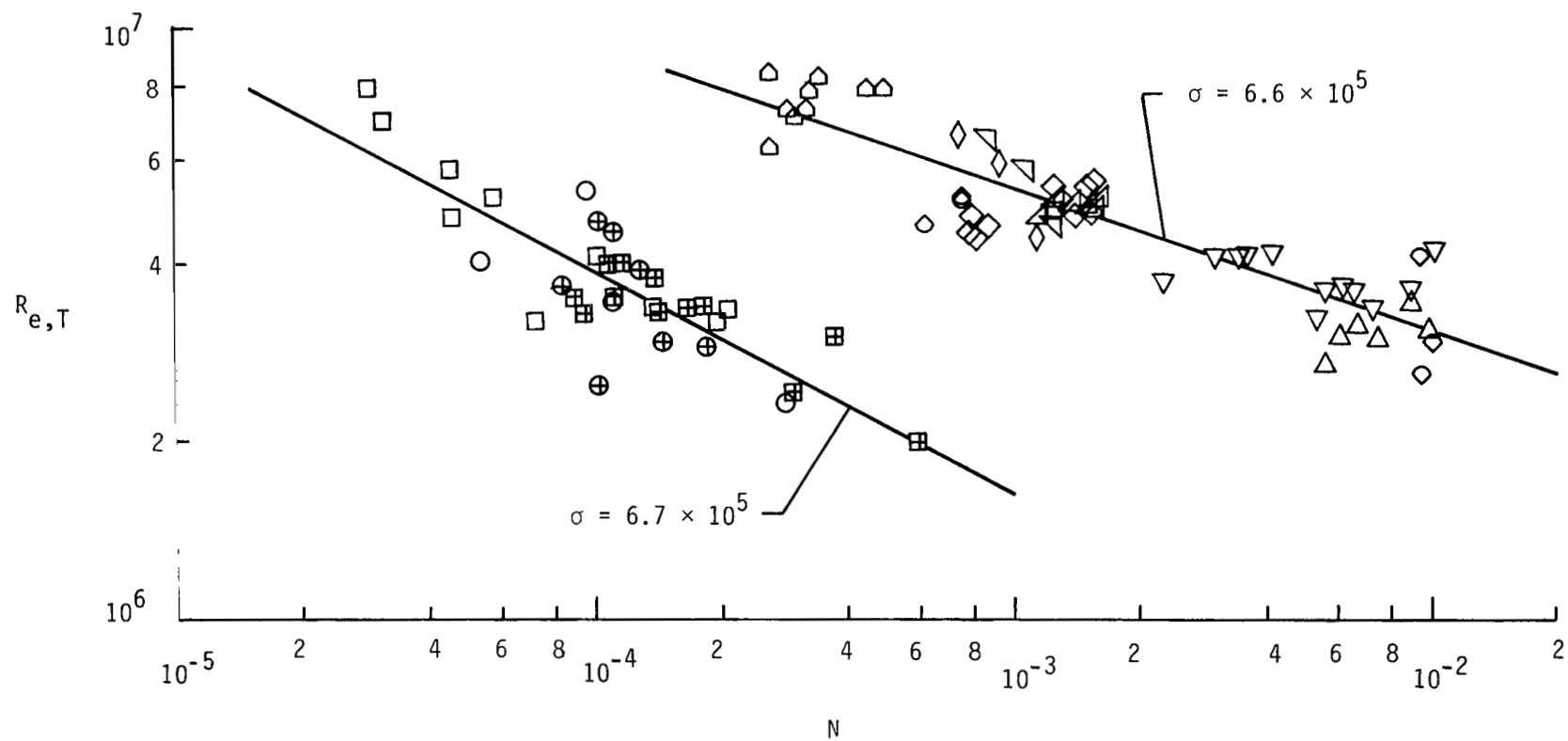
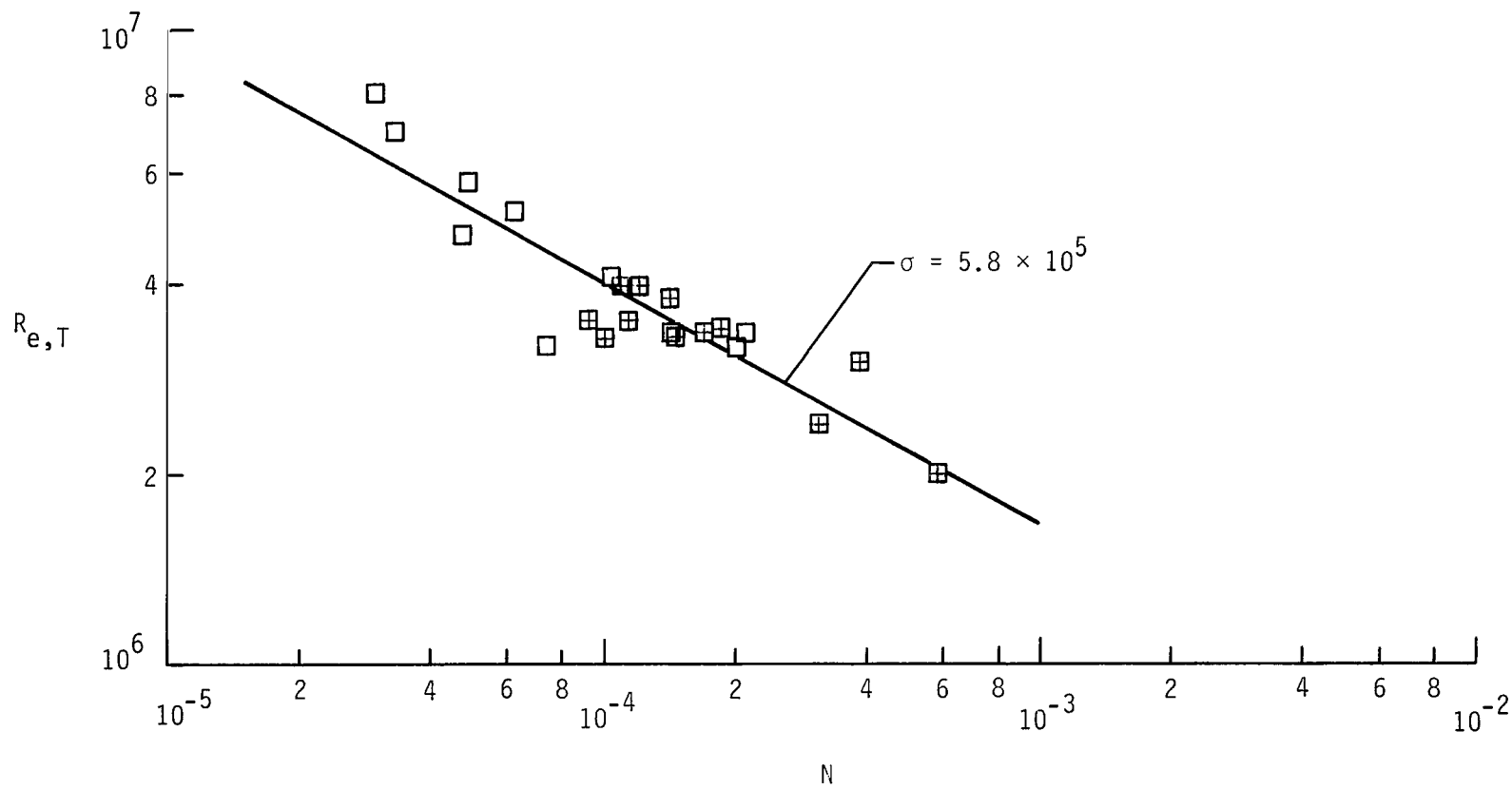


Figure 7.- Correlation of $R_{e,T}$ with N where $N = \frac{1}{s_T} \left[\int_0^{s_N} \frac{\tilde{p}}{\tilde{q}} \frac{F_m R_\infty}{0.25} ds + 13 \int_{s_N}^{s_T} \frac{\tilde{p}}{\tilde{q}} \exp \left(-13 \frac{s - s_N}{s_T - s_N} \right) \frac{F_m R_\infty}{0.25} ds \right]$.
 Data symbols are defined in table IV.



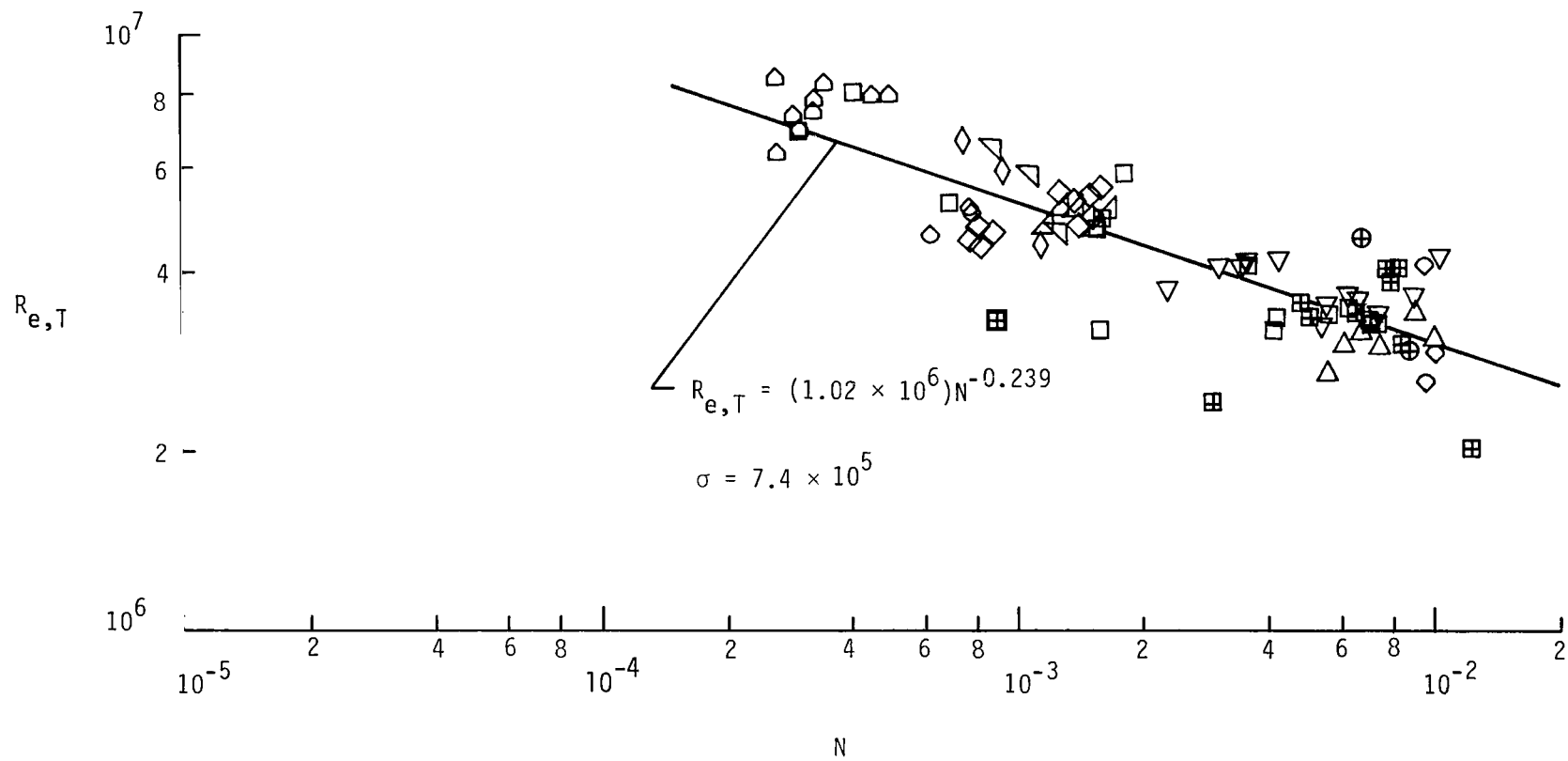
$$(a) \quad N = \frac{14}{s_T} \int_0^{s_T} \frac{\tilde{p}}{\tilde{q}} \exp\left(-14 \frac{s}{s_T}\right) ds.$$

Figure 8.- Correlation of $R_{e,T}$ with N . Data symbols are defined in table IV.



$$(b) \quad N = \frac{13}{s_T} \int_0^{s_T} \frac{\tilde{p}}{q} \exp\left(-13 \frac{s}{s_T}\right) ds.$$

Figure 8.- Continued.



$$(c) \quad N = \frac{10}{s_T} \int_0^{s_T} \frac{\tilde{p}}{q} \exp\left(-10 \frac{s}{s_T} \frac{F_m R_\infty}{0.25}\right) ds.$$

Figure 8.- Concluded.

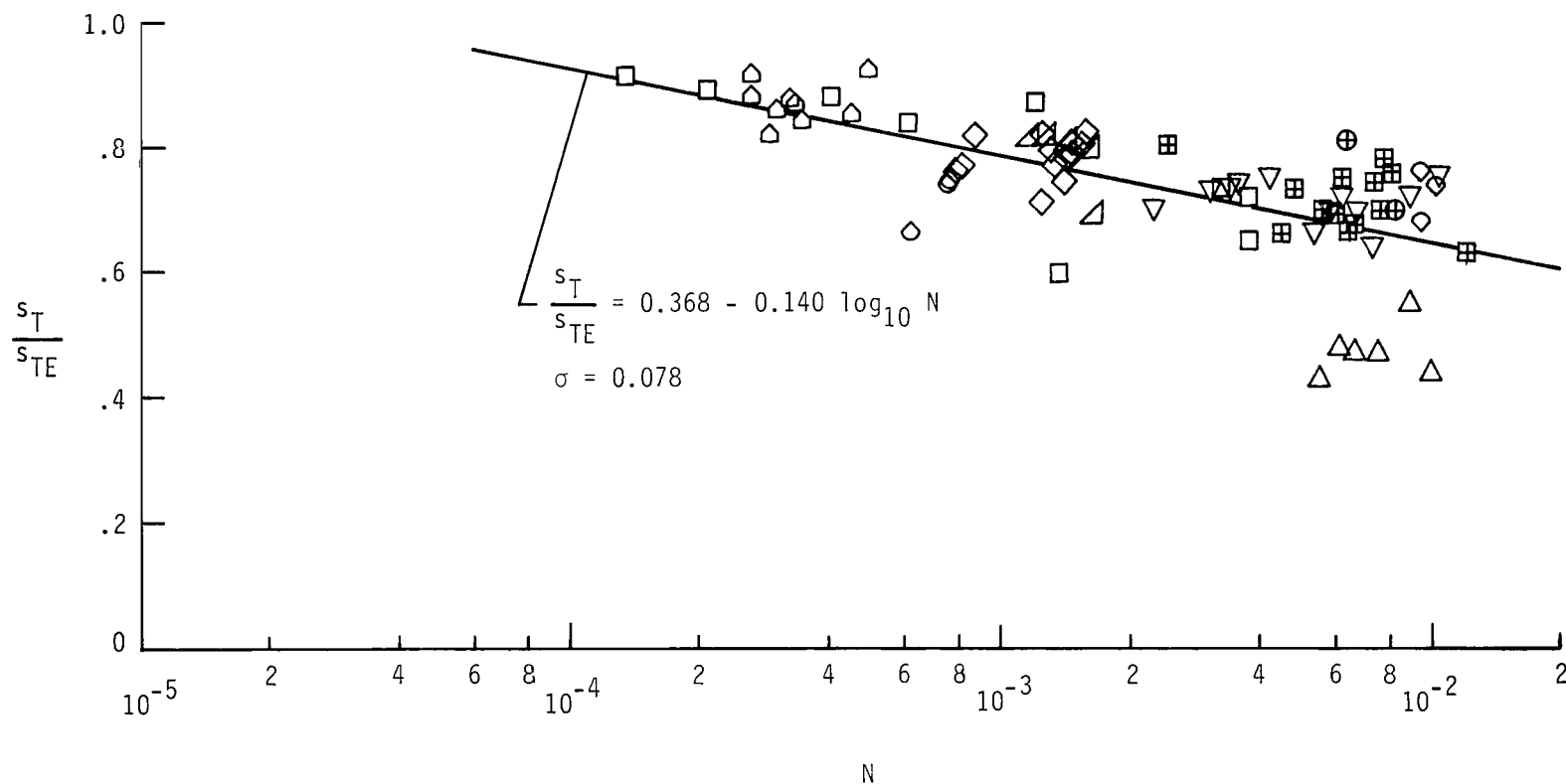


Figure 9.- Correlation of $\frac{s_T}{s_{TE}}$ with N where $N = \frac{13}{s_T} \int_0^{s_T} \frac{\tilde{p}}{q} \exp\left(-13 \frac{s}{s_T}\right) \frac{F_m R_\infty}{0.25} ds$. For the data symbol \oplus , $R_\infty = 7.0 \times 10^5$ per inch for the PQ tunnel with axisymmetric nozzle (B.V. closed). For all other symbols, see table IV.

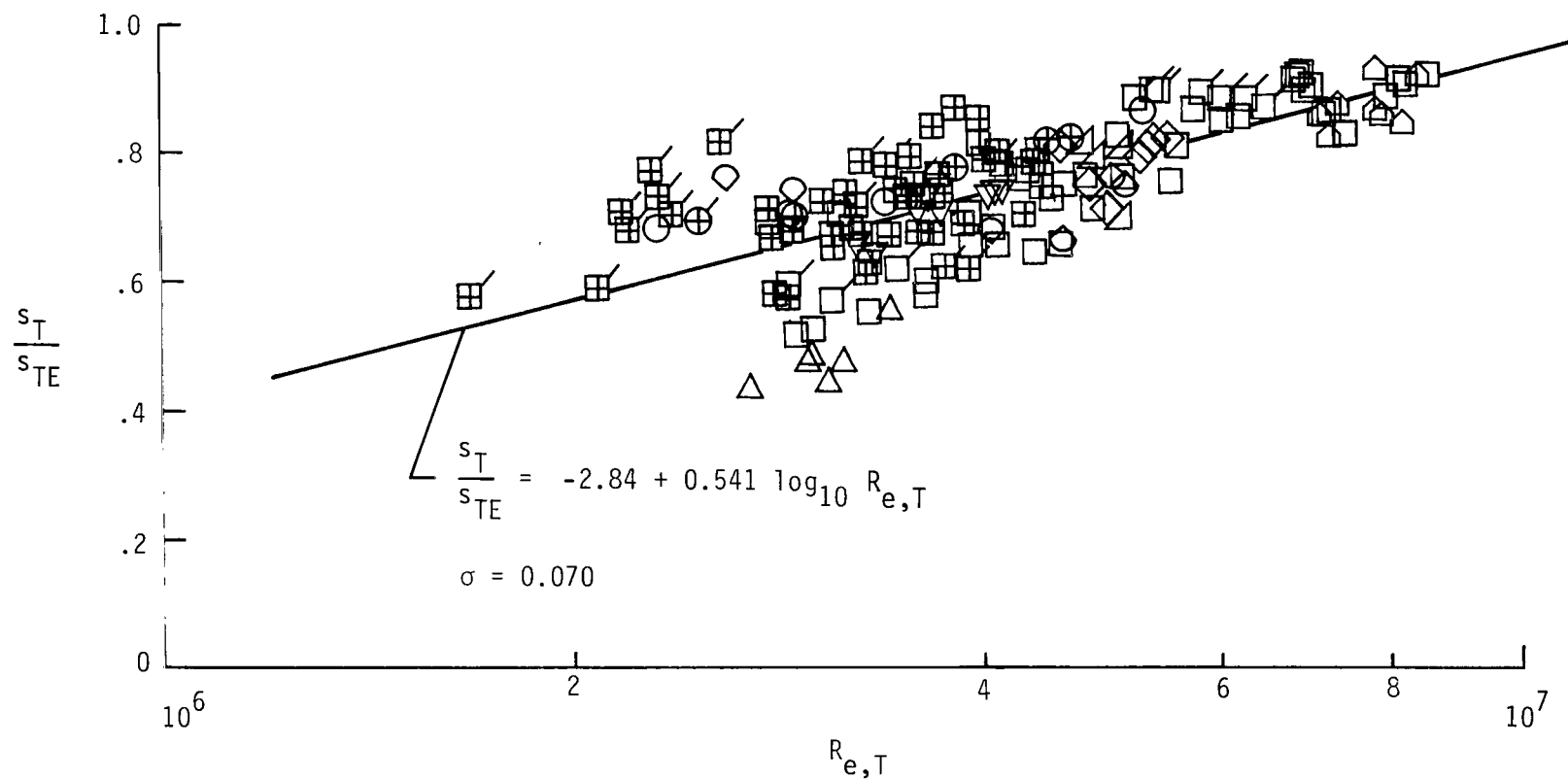


Figure 10.- Correlation of $\frac{s_T}{s_{TE}}$ with $R_{e,T}$. Flagged symbols indicate data for cones in downstream location. Data symbols are defined in table IV.

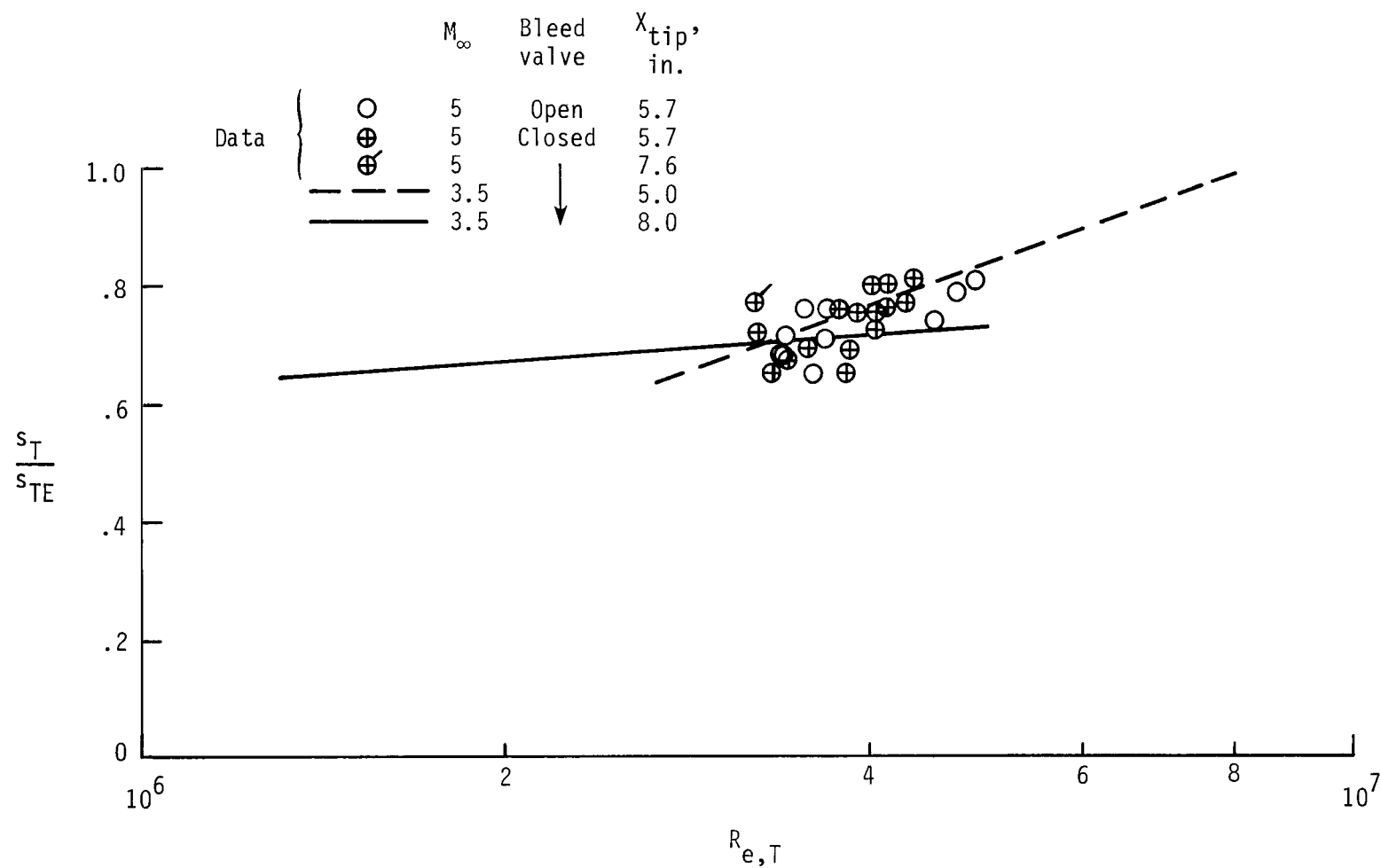


Figure 11.- Comparison of data from the Mach 5 pilot quiet tunnel and correlation lines for data from the Mach 3.5 pilot quiet tunnel.

1. Report No. NASA TP-2229		2. Government Accession No.		3. Recipient's Catalog No.	
4. Title and Subtitle CORRELATIONS OF SUPERSONIC BOUNDARY-LAYER TRANSITION ON CONES INCLUDING EFFECTS OF LARGE AXIAL VARIATIONS IN WIND-TUNNEL NOISE				5. Report Date January 1984	
7. Author(s) Fang-Jenq Chen, Ivan E. Beckwith, and Theodore R. Creel, Jr.				6. Performing Organization Code 505-31-13-05	
9. Performing Organization Name and Address NASA Langley Research Center Hampton, VA 23665				8. Performing Organization Report No. L-15669	
12. Sponsoring Agency Name and Address National Aeronautics and Space Administration Washington, DC 20546				10. Work Unit No.	
15. Supplementary Notes Fang-Jenq Chen: Systems and Applied Sciences Corporation, Hampton, Virginia. Ivan E. Beckwith and Theodore R. Creel, Jr.: Langley Research Center, Hampton, Virginia.				11. Contract or Grant No.	
16. Abstract Transition data on sharp-tip cones in two pilot low-disturbance wind tunnels at Mach numbers of 3.5 and 5 have been correlated in terms of noise parameters with data from several conventional wind tunnels and with data from supersonic flight tests on the Arnold Engineering Development Center transition cone. The noise parameters were developed to account for the large axial variations of the free-stream noise and the very-high-frequency noise spectra that occurred in the low-disturbance tunnels for some test conditions. The noise could be varied in these tunnels from high levels, approaching those in conventional tunnels, to extremely low levels. The correlations indicated that transition in the low-disturbance tunnels was dominated by the local stream noise that was incident on the cone boundary layer upstream of the neutral stability point. The correlation results also suggested that high-frequency components of the low-disturbance-tunnel noise spectra had significant effects on transition when the noise was incident on the boundary layer both upstream and downstream of the neutral stability point.				13. Type of Report and Period Covered Technical Paper	
17. Key Words (Suggested by Author(s)) Supersonic wind tunnel Free-stream noise Transition Boundary layer				14. Sponsoring Agency Code	
18. Distribution Statement Unclassified - Unlimited Subject Category 34					
19. Security Classif. (of this report) Unclassified	20. Security Classif. (of this page) Unclassified	21. No. of Pages 54	22. Price A04		

National Aeronautics and
Space Administration

Washington, D.C.
20546

Official Business

Penalty for Private Use, \$300

THIRD-CLASS BULK RATE

Postage and Fees Paid
National Aeronautics and
Space Administration
NASA-451



2 1 10, D. 840120 S00903DS
DEPT OF THE AIR FORCE
AF WEAPONS LABORATORY
ATTN: TECHNICAL LIBRARY (SUL)
KIRTLAND AFB NM 87117

NASA

POSTMASTER:

If Undeliverable (Section 158
Postal Manual) Do Not Return